THE ROLE OF *atg18* IN SIGNAL TRANSDUCTION PATHWAYS DURING *DROSOPHILA* DEVELOPMENT

by

Erica L. Boetefuer

A thesis submitted to the Faculty of the University of Delaware in partial fulfillment of the requirements for the degree of Honors Bachelor of Science in Biological Sciences with Distinction

Spring 2012

THE ROLE OF *atg18* IN SIGNAL TRANSDUCTION

PATHWAYS DURING *DROSOPHILA* DEVELOPMENT

by

Erica L. Boetefuer

Approved: _____

Dr. Erica M. Selva, Ph.D
Professor in charge of thesis on behalf of the Advisory Committee

Approved: _____

Dr. David W. Smith, Ph.D
Committee member from the Department of Biological Sciences

Approved: _____

Dr. Meredith C. Wesolowski, Ed.D
Committee member from the Board of Senior Thesis Readers

Approved: _____

Michael Arnold, Ph.D.
Directory, University Honors Program

ACKNOWLEDGMENTS

Pursuing research and writing an undergraduate senior thesis has been a truly rewarding experience that has allowed me to take full advantage of my time at the University of Delaware. My success with this undertaking would not have been possible without support from several people. First and foremost I would like to thank my mentor, Dr. Erica M. Selva. Dr. Selva served as not only my research mentor but also my academic advisor. I have truly enjoyed working with Dr. Selva and cannot thank her enough for all she has done for me in helping to achieve my goals. I could not have gotten through this process without her guidance and mentorship. I have also had the support of an incredible lab group who have taught me so much and have also become great friends. Net, Alicia, Allison, Scott, Sencer, Babak, and Nick: I have enjoyed getting to know each one of you and I am going to miss working with you! Thank you for all of the great times! I would also like to thank my committee, Dr. David W. Smith and Dr. Meredith C. Wesolowski for their support. You helped make this process run very smoothly and I appreciate all you have done for me. I would like to say a huge thank you to Mom, Dad, and Laura, as well as the rest of my family for their full support through this whole process. I have been lucky enough to also have the support from a great group of friends who have helped me in so many ways. Finally, I would like to thank the University of Delaware Undergraduate Research Program and Howard Hughes Medical Institute for the opportunity to pursue research and for the amazing experiences I have had throughout the entire course of my undergraduate career.

TABLE OF CONTENTS

LIST OF TABLES

LIST OF FIGURES

ABSTRACT

8J16 and 9E6 are allelic mutations that disrupt Wnt/Wingless (Wg) or Hedgehog (Hh) signaling based upon their embryonic 'lawn of denticles' phenotype. Goals of this project were to identify the disrupted gene and determine its role in *Drosophila* developmental signaling. Complementation analysis revealed 8J16/9E6 are alleles of autophagy-specific gene 18, *atg18*, which plays a role in autophagosome-lysosome fusion. In yeast, *atg18* negatively regulates endosome-vacuole targeting, the yeast lysosomal equivalent. In *Drosophila,* endocytic machinery mutations that block lysosome targeting cause continuous signaling. Therefore, I hypothesized *atg18* mutants should cause a buildup of lysosomes at the expense of endosomes and decrease signaling. To the contrary, Distalless (Dll), a long-range Wg target, was enhanced in 8J16/9E6 mutant tissue in *Drosophila* wing discs. Analysis of 8J16/9E6 germline clone (glc) mutant embryos confirmed $atg18^{8J16}$, $atg18^{9E6}$, and $atg18^{KG03090}$ ($atg18^{P}$) are allelic. Immunofluorescent staining of glc embryos showed the segmentation defect is due to loss of Wg expression at embryonic stage nine. 8J16/9E6 glc embryos also display severe CNS defects not strictly the result of Wg loss and thus, these mutation show pleiotropic effects. 8J16/9E6 are intronic point mutations not predicted to disrupt mRNA splicing. Additionally, mutants are temperature sensitive, yielding lethality at 25ºC, but are partially viable at 29ºC. qPCR revealed a decrease in *atg18* transcript levels in 8J16/9E6 relative to wild type (WT). At the increased temperature, an average five-fold reduction was found in WT *atg18* transcripts levels. Relative to WT, 8J16/9E6

show a slight increase of *atg18* transcript levels at 29ºC, which may explain the rescue phenotype observed at this temperature in the mutants. In order to further address the effect of this temperature sensitivity on signaling in wing discs, clonal analysis was performed using a non-heat shock system, which may show evidence of a decrease in signaling in 8J16/9E6 mutant tissue. Further experiments are required to fully characterize these mutants and the mechanisms by which they are acting to cause these disrupted phenotypes.

Chapter 1

INTRODUCTION

1.1 The 8J16 and 9E6 Mutants

8J16 and 9E6 are two independent *Drosophila melanogaster* allelic mutants generated previously using ethylmethane sulfonate (EMS) random mutagenesis and identified via an embryonic screen. The 'lawn of denticles' embryonic cuticle phenotype generated by these mutations suggests that the disrupted gene plays a role in the Wingless (Wg) or Hedgehog (Hh) signal transduction pathway during *Drosophila* development (Figure 1) (Selva & Stronach, 2007). The long-term goal of this project is to clone and characterize the 8J16 and 9E6 mutations, focusing on examining how the wild type gene product modulates signaling in developing organisms.

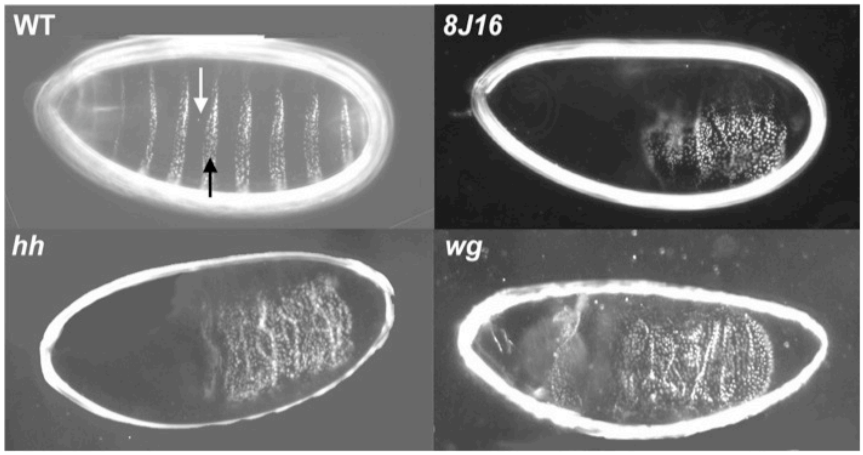

Figure 1. **Comparison of the 8J16 terminal embryonic cuticle phenotype to Hh and Wg mutants.** Hh and Wg signaling pathways are required for the deposition of naked cuticle (white arrow in wild type, WT) in the embryo. Black arrow indicates denticle bands. Mutations that disrupt either pathway yield a 'lawn of denticles' phenotype. The 8J16 and 9E6 mutations yield the same 'lawn of denticles' phenotype, suggesting they disrupt Hh or Wg signaling. Images are taken in darkfield with the vitelline membranes intact (Figure adapted from Selva & Stronach, 2007).

1.2 Wingless and Hedgehog Signaling Pathways

Organism growth and development and adult homeostasis are all complex processes that rely on the activation and maintenance of highly conserved signal-transduction pathways by extracellular signals (Goodman et al., 2006). The Wnt/Wingless (Wg) and Hedgehog (Hh) signaling pathways are two such pathways that play a critical role throughout various stages of development as well as during adult homeostasis. *Wnt* genes are highly conserved genes present in all metazoan with 20 known Wnt proteins in mammals (Clevers, 2006). The best-characterized Wnt is the *Drosophila* Wg, which was originally discovered in *wg* mutant flies that lacked or had malformed wings. The *hh* gene family contributes Hh signaling proteins, for which there are three human paralogs (Geissler & Zach, 2012). These signaling

pathways are highly regulated and involve the secretion of the ligand, Wg or Hh, to act upon short- or long-range neighboring cells in a diffusion gradient-dependent manner. When the secreted signal protein is recognized by the target cell a signaling cascade is activated, resulting in the expression of downstream target genes expressed in these cells (Taipale & Beachy, 2001).

As shown in Figure 1, *wg* and *hh* are both required during embryogenesis for proper segmentation of the embryo and are therefore known as segment polarity genes. In early embryogenesis, *hh* is expressed in a banded fashion in epidermal cells in response to the transcription factor Engrailed (En). The Hh ligand is then secreted to adjacent cells, where it activates *wg* expression. The secreted Wg ligand then signals posterior epidermal cells to maintain *en* expression (Selva & Stronach, 2007). Together, this signaling feedback loop determines embryonic segmentation (Figure 2) (Lin, 2004).

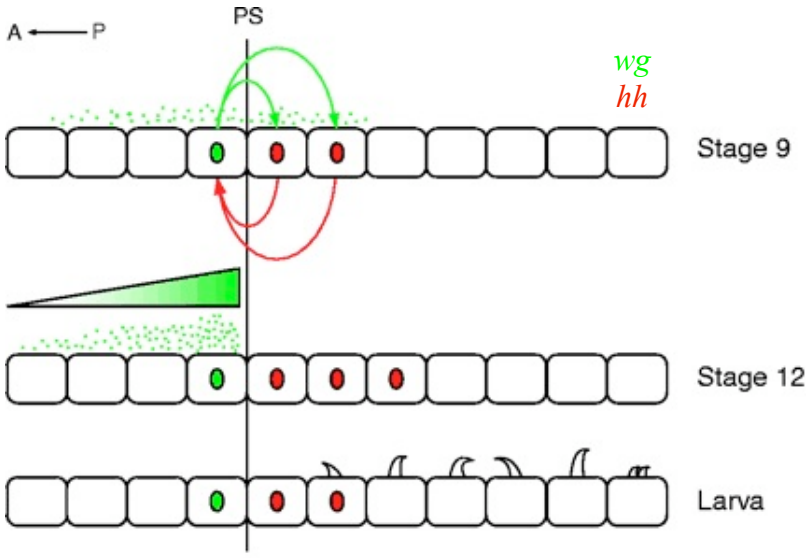

Figure 2. **Wg and Hh work in a feedback loop for the deposition of naked cuticle in embryos**. During embryogenesis, *wg* (green) and *hh* (red) act in a feedback loop. At embryonic stage nine Hh signals anteriorly to maintain *wg* expression, which allows Wg to signal posteriorly and maintain *hh* expression. By stage 12, anteriorly distributed Wg forms a gradient required for larval naked cuticle deposition. Alternating segments in larvae contain denticles, small hairs on the surface of the cuticle. Loss of Wg or Hh signaling results in the 'lawn of denticles' patterning defect seen in Figure 1 (Figure adapted from Lin, 2004).

In addition to the role of Wingless (Wg) and Hedgehog (Hh) during embryonic development, the Wg and Hh signaling pathways are also involved in later stages of *Drosophila* development, and are key regulators required throughout the adult life (Clevers, 2006). In later developmental stages, Wg and Hh are required for patterning of the imaginal discs, which develop into adult structures (see section 2.3) (Geissler & Zach, 2012). In vertebrates, Wnt signaling is involved in brain, kidney, placenta, hindgut, and limb development as well as stem cell homeostasis. Human Hh is required for embryogenesis, limb and neural tube patterning, brain development, and tissue regeneration (Geissler & Zach, 2012). Loss of Hh in humans has been

associated with defects in development and adult malformations (Taipale & Beachy, 2001). Aberrant Wnt and Hh signaling has been shown to play a pathological role in numerous human diseases, including colon, ovarian, intestinal, skin, lung, pancreatic, breast and prostate cancers (Geissler & Zach, 2012). In some adult tissues Wnt and Hh play a role in homeostasis by regulating somatic stem cell numbers, which is especially important in tissues with cells undergoing constant renewal, such as skin and intestinal epithelial cells. Because of the similarity of stem cell properties to that of tumor cells (most notably the ability to self-renew and maintain nearly unlimited replication), it has been suggested that the expansion of these stem cell populations may be the first step in tumorigenesis (Taipale & Beachy, 2001). Due to the role of aberrant Wg or Hh signaling as a key mechanism for the development of many known diseases, these signaling pathways are readily being targeted in the development of new therapeutics, especially those focusing on human cancers (Geissler & Zach, 2012).

1.3 *Autophagy-specific Gene 18*

After the mutants were shown to play a role in Wg or Hh signaling, efforts sought to identify the gene disrupted by 8J16 and 9E6 mutations. Complementation analysis comparing mutants to known deficiencies narrowed the region in which the disrupted gene is located to between 66B8 and 66B11 on the left arm of chromosome three. Of the ten genes located within this region, complementation analysis was performed on five of these genes, which revealed that 8J16 and 9E6 are novel alleles of *autophagy-specific gene 18*, denoted from this point forward as simply *atg18* (Figure 3).

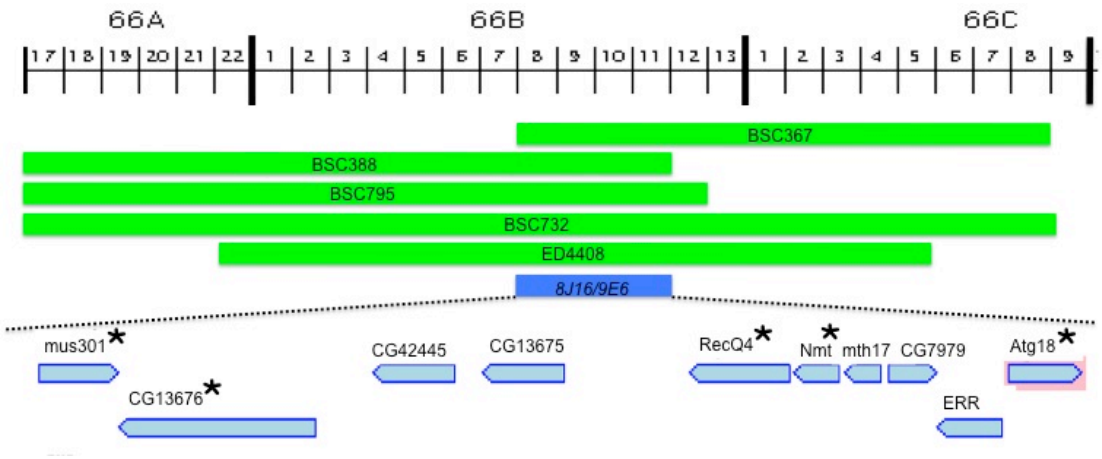

Figure 3. **Complementation analysis delineating the discovery of *atg18* as the gene disrupted by 8J16 and 9E6 mutations.** Regions absent in deficiencies are shown as solid bars. Green denotes non-complementation, therefore 8J16/9E6 are between 66B8 and 66B11 on the left arm of chromosome three, the region of overlap. Mutants did complement BSC815 (not shown), a deficiency just outside of this region. Complementation analysis to five of the ten genes within this region (marked with asterisks) identified 8J16 and 9E6 as two novel alleles of *atg18*. An independent mutation in *atg18* did not complement the 8J16 or 9E6 mutations (work done by Andrea Short, 2007).

Drosophila atg18 is a 3,714 base pair long, protein-coding gene containing five exons and four introns. The protein coded for by this gene is 377 amino acids in length and contains motifs homologous to the WD40 repeat. This repeat has been shown in all eukaryotes to play a wide variety of roles, including the regulation of signal transduction pathways, transcription, cell cycle checkpoints, and protein-protein interactions. *atg18* homologs are present in many additional species, including yeast and human (*WIPI-2*) (FlyBase, 2012). In *Drosophila*, the exact molecular function of *atg18* is unknown, yet it has been shown to play a role in autophagy (Berry & Baehrecke, 2007). Autophagy is a general term used to describe the degradation of

cytoplasmic contents in lysosomes. This is a highly regulated, highly conserved process involved in the starvation response, protein and organelle turnover, development, aging, microorganism elimination, tumor suppression, and cell death. Autophagy is categorized by the formation of the autophagosome, which begins with the sequestration of cytoplasmic contents to a phagophore. This structure then fuses with the lysosome, creating the autolysosome and allowing content degradation (Figure 4). Though this process is distinct from the endocytic degradation pathways, endosomes also regularly fuse with autophagosomes before fusing with the lysosome. After degradation in the lysosome, broken down macromolecules may be exported to the cytosol for reuse (Mizushima, 2007).

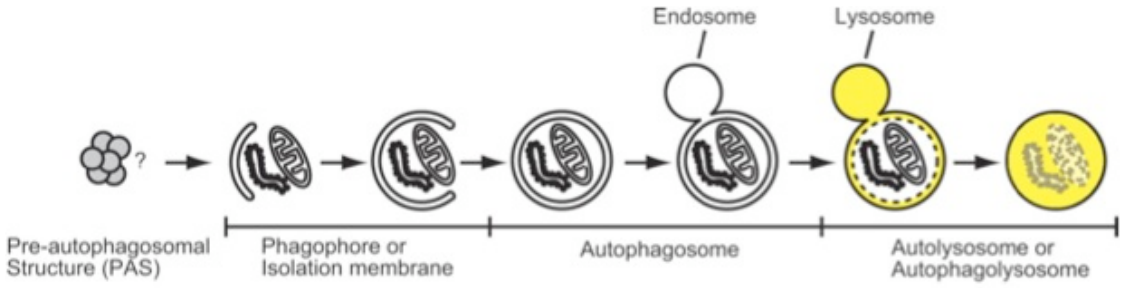

Figure 4. **The process of autophagy**. The formation of the autolysosome during autophagy involves sequestration of cytoplasmic contents into a phagophore, formation of the autophagosome and subsequent fusion with the lysosome, which allows for content degradation (Figure adapted from Mizushima, 2007).

The exact molecular function of *atg18* has not been fully characterized in *Drosophila*. Therefore, a hypothesis of the role of mutations within *atg18* was based on both the gene function in yeast as well as observations made in *Drosophila*. It has

been shown that phosphatidylinositol 3 (PI3)-kinases function as regulators of autophagy (Rusten et al., 2006). Specifically, *fab1* and *atg18* have both been shown to play a role in endosome maturation and lysosome fusion. Fab1 is a lipid kinase that phosphorylates phosphatidylinostiol 3-phosphate [PtdIns(3)P] into phosphatidylinositol-3,5-bisphosphate [PtdIns(3,5)P_2]. These two molecules are characteristic of and distinguish early and late endosomes, with PtdIns(3)P found in early endosomes and PtdIns(3,5)P_2 found in late (Efe, Botelho, & Emr, 2007). In the late endosome, PtdIns(3,5)P_2, and therefore *fab1*, is required for the sorting of membrane vesicles via protein receptors that interact with membrane lipids for trafficking to the lysosome and degradation (Rusten et al., 2006). As shown in Figure 5, Atg18 is an effector molecule that senses PtdIns(3,5)P_2 and acts as a negative regulator of Fab1. Triggered by an increase in the product of Fab1 function [PtdIns(3,5)P_2,], Atg18 is directed to the Fab1 complex, turns off Fab1 kinase, halts phosphorylation, and decreases PtdIns(3,5)P_2 (Efe et al., 2007).

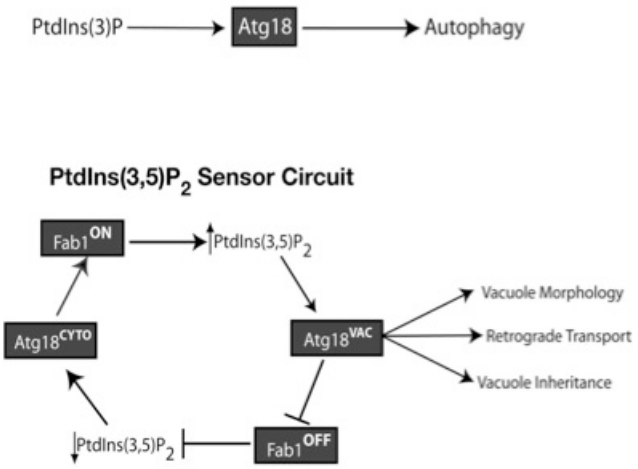

Figure 5. **Regulation of Fab1 by Atg18 in yeast.** Atg18 responds to changes in PtdIns(3,5)P_2 via a negative feedback loop with Fab1 (Figure adapted from Efe et al., 2007).

Yeast *atg18* functions as a negative regulator in the fusion of endosomes to the vacuoles, the equivalent of lysosomes, was shown by an increase in endosomal targeting to the vacuoles in cells lacking *atg18* (Efe et al., 2007). An important observation in *Drosophila* is that mutations in the endocytic machinery that block lysosomal targeting result in continuous signaling, leading to hyperactivation of mitogenic signaling pathways (Rusten et al., 2006). Taken together, I hypothesize that mutations within *Drosophila atg18* will drive the endocytic pathway toward the lysosome, thereby decreasing signaling within *atg18* mutants.

1.4 Greater Initiative

Research being conducted on these two mutants is part of a greater initiative aimed towards gaining a further understanding of the roles of cellular components in Wg and Hh signaling pathways. Because these two pathways are required for

numerous phases of *Drosophila* development as well as for adult homeostasis, conducting experiments on various mutants that show phenotypes consistent with loss of Wg or Hh signaling and examining their effects on essential cellular components may aid in the discovery of key mechanisms regulating cell signaling. The goal of these experiments is to identify the gene disrupted by 8J16 and 9E6, the means by which these mutations affect signaling and cause an abnormal phenotype, and the specificity of these pathways. Abnormalities in both signaling and autophagy have been implicated in various human diseases, and examining a connection between these two processes may bring light to a novel mechanism of disease regulation.

1.5 Specific Aims

Both 8J16 and 9E6 mutations show a phenotype indicative of a block in Wg or Hh signaling. By examining these mutations, the goal of this research is to determine how signaling is disrupted and the molecular mechanism by which these mutations cause a phenotype. The specific aims of this research are as follows:

Specific Aim 1: Test whether *agt18* mutant tissue in the developing *Drosophila* wing disc leads to an increase in the lysosomal compartment and a reduction in endocytic vesicles.

Specific Aim 2: Determine if there is a decrease in targets of Wg, Hh, and other signaling pathways within *atg18* mutant tissue.

Specific Aim 3: Characterize the mechanisms by which these mutations affect signaling and cause a disrupted phenotype as well as determine the specificity of the pathway by which the mutants achieve this phenotype.

Chapter 2

METHODS AND MATERIALS

2.1 General *Drosophila* Protocols

Generally, flies were kept in vials of prepared food media (agar, yeast, sugar and cornmeal), Carolina™ Blue Food and yeast at 25ºC in mild humidity. Stocks were maintained by flipping flies into fresh vials every ten days. For experimental crosses, flies were kept at 18°C and collection of virgin females was performed twice daily. Males could be selected any time between adult days two and ten. Experimental crosses were expanded by transferring vials every four days. Collections and observations of flies were performed using CO_2.

2.2 *Drosophila* as a Model Organism

Drosophila melanogaster is a widely used model organism in many different fields of biology ranging from cell biology to neurobiology to development to pathology of human diseases. The popularity of *Drosophila* as a model organism comes from the ability to combine classical genetics with a variety of cellular, molecular, and biochemical techniques in order to study complex biological processes. The complete genome sequence is known and the analysis of this information is progressing rapidly, advancing studies using this system (Fernández-Moreno, Farr, Kaguni, & Garesse, 2007). *Drosophila* genetics are the classical model system for performing these studies and extensive research has elucidated countless advantages to the tools available within this system. One such genetic tool key to this model system

is the use of balancer chromosomes, which are highly rearranged chromosomes containing a dominant visible marker. These dominant markers are used to identify targeted progeny of crosses as they result in a visible phenotype in the offspring receiving the balancer. Balancer chromosomes are also utilized to prevent homologous recombination events, preserving mutated chromosomes (Fernández-Moreno et al., 2007).

Another advantage to using *Drosophila* as a model system in research is the short duration of the life cycle. The generation time is, on average, around ten days from fertilized egg to eclosed adult when kept at 25°C. With such a short life cycle and large number of offspring produced by each female (~100 embryos/day), there is a great opportunity for examining these individuals using various genetic, biochemical, and molecular techniques. The *Drosophila* life cycle consists of four stages: embryo, larva, pupa, and adult (Figure 6). Embryogenesis lasts only 24 hours. The larval stage lasts approximately three days and consists of two molts that allow the larvae to progress from first to second then second to third instar larvae. Third instar larvae prepare for pupation by moving up the walls of the vials. Pupation lasts approximately four days, during which time a complete metamorphosis takes place and adult organs develop from the imaginal discs present in the larvae (Figure 7). These discs have been the subject of many studies that examine genes involved in development into the adult, which emerges around post-fertilization day ten (Fernández-Moreno et al., 2007).

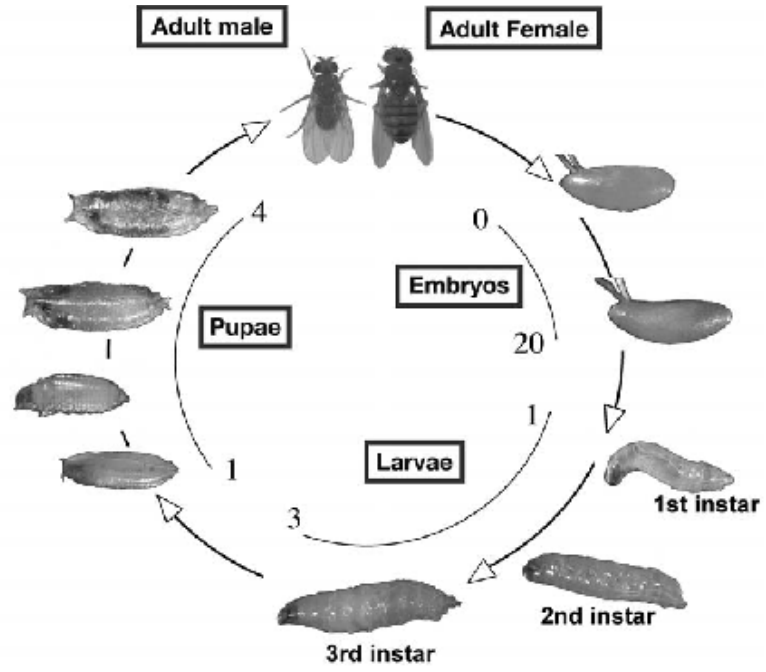

Figure 6. **A timeline of the *Drosophila* life cycle.** The time from fertilization to eclosure of the adult fly is approximately ten days (Fernández-Moreno et al., 2007).

2.3 Methods for Experiments on *Drosophila* Wing Imaginal Discs

Though initial characterization of 8J16 and 9E6 that showed a loss of Wg/Hh signaling was performed in embryos, examination of signaling defects was also performed at later stages of *Drosophila* development. During larval stages, *Drosophila* contain several imaginal discs that later develop into various structures of the adult fly (Figure 7). The wing imaginal disc, the largest of these discs, develops into the adult wing and is an ideal system for studying signaling during development.

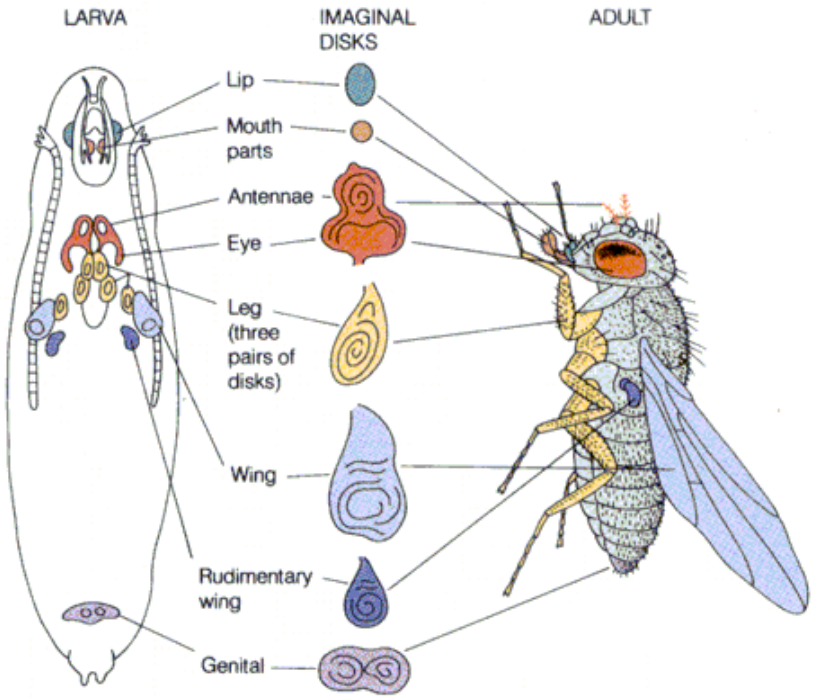

Figure 7. ***Drosophila*** **larvae contain imaginal discs that develop into adult structures.** These discs are often utilized to study developmental processes. This project focuses specifically on signaling in the wing imaginal disc during development (Figure adapted from Mathews & Van Holde, 1990).

For this study wing discs are an appropriate tissue to examine because Wg and Hh, which function in a feedback loop during embryonic stages, function independently during wing development and can therefore be distinguished in wing discs. Additionally, previous mutations showing the same embryonic "lawn of denticles" phenotype have been shown to disrupt signaling in the wing discs (Goodman et al., 2006). Wing discs also have advantages for studying signaling defects as there many signaling pathways activated within the wing disc during development, which have well characterized downstream targets that may be easily

examined (Lin, 2004). In the wing disc, Wg is secreted from the dorsal-ventral (DV) boundary and signals into the dorsal and ventral compartments (Lin, 2004), activating downstream targets such as Achaete (Ac) and Distalless (Dll) (Taipale & Beachy, 2001). Hh is expressed in the posterior compartment and signals into the anterior compartment (Lin, 2004), activating downstream targets such as Patched (Ptc) (Figure 8) (Taipale & Beachy, 2001). These signaling pathways are required for proper disc patterning and adult wing development (Lin, 2004). Using antibodies to visualize these signaling molecules and their targets, wing discs provide an ideal model system by which signaling can be studied.

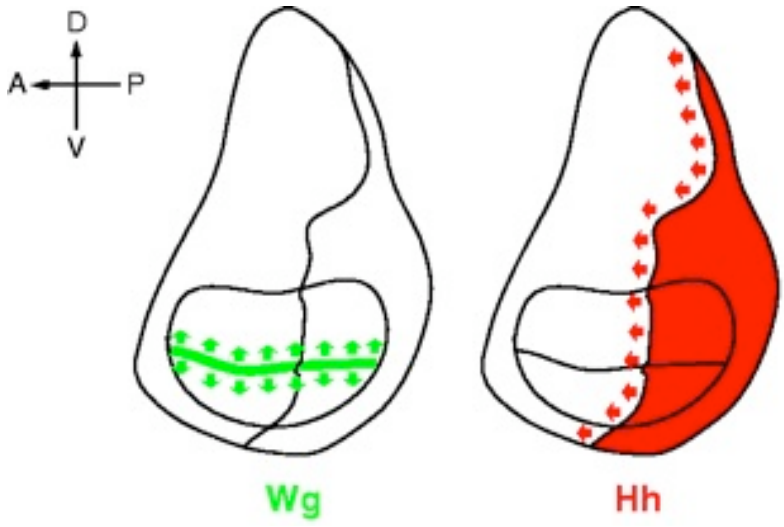

Figure 8. **Signaling pattern of Wg and Hh in the *Drosophila* wing disc.** Wg is expressed along the DV boundary and signals into the dorsal and ventral compartments, while Hh is expressed in the posterior compartment and signals anteriorly. Expressed in the wing disc of third instar larvae, these morphogen signaling gradients are required for wing imaginal disc patterning and adult wing development (Figure adapted from Lin, 2004).

Another technique, and perhaps the most powerful tool, that can be employed in the wing discs is the ability to create mosaic clones, which allows a side-by-side analysis of mutant tissue to wild type tissue using the FRT/FLP recombination technique, shown in Figure 9 (Theodosiou & Xu, 1998).

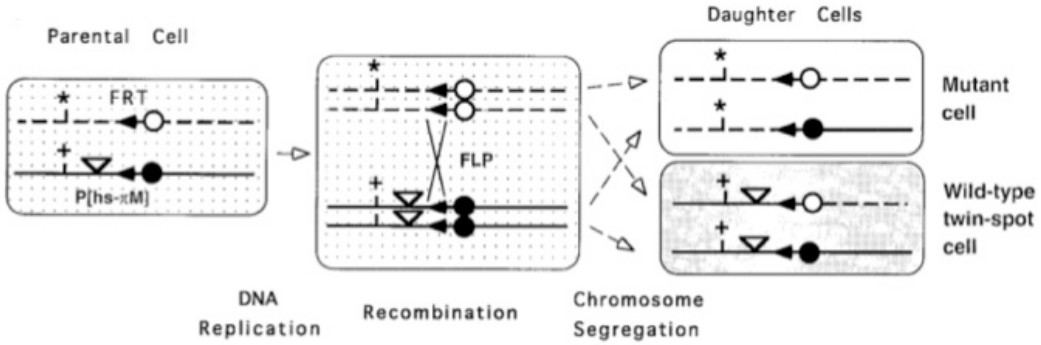

Figure 9. **FLP/FRT recombination is utilized to induce mitotic recombination.** After DNA replication under heat shock activation the yeast site-specific recombinase FLP induces mitotic recombination in a heterozygous parental cell at the target FRT site (black arrowhead). Following chromosome segregation, resulting cells can possess either wild type (+) or mutant (*) chromosomes. Further divisions result in clones from each of these daughter cells, which can be distinguished via a cell marker (white arrowhead) (Figure adapted from Theodosiou & Xu, 1998).

For these experiments, the recombination between FRT sites of homologous chromosomes was induced via a heat shock promoter, which was induced by moving vials to 37°C for one hour on day three after egg laying. Green fluorescent protein (GFP) is utilized as a marker of recombination. Randomly generated mutant clones in the wing disc are denoted by the absence of GFP, while positive GFP marks wild type

tissue (Figure 10). The expression of GFP was induced by an additional one-hour heat shock at 37°C on day seven just prior to dissection.

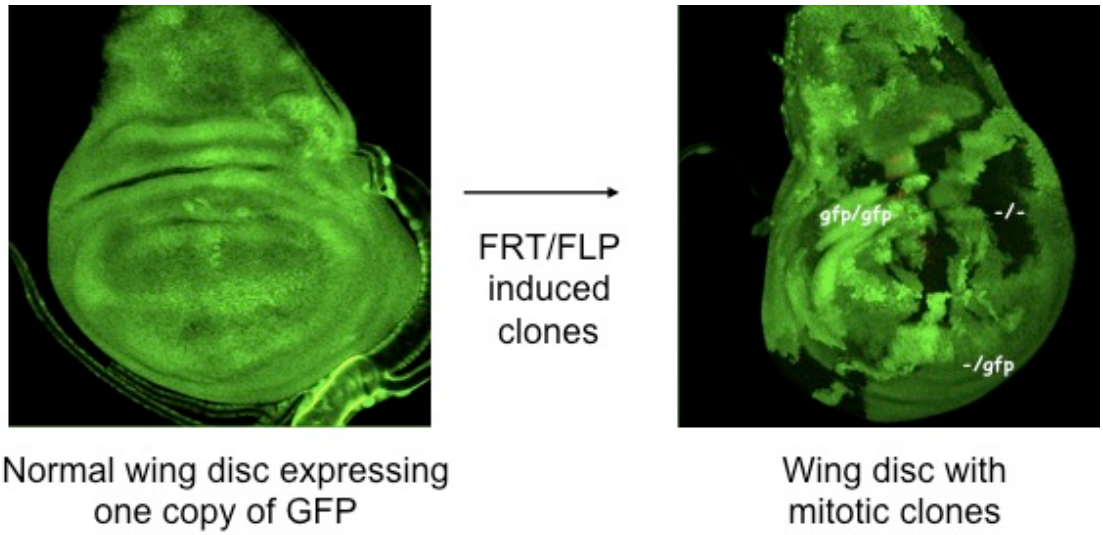

Figure 10. **Side-by-side clonal analysis using a GFP marker.** GFP is utilized as a cell marker in the FLP/FRT recombination system. GFP segregates with the wild type gene while the absence of GFP marks mutant tissue.

In order to examine the effects of the 8J16 and 9E6 mutations on signaling molecules, downstream signaling targets, and intracellular compartments, wing imaginal discs were isolated from third instar larvae utilizing the system depicted in Figure 10. Virgin *yw hsFlp/yw hsFlp; m^{i55} hsGFP FRT^{2A}/TM6B* females were collected and crossed to mutant males, ♂*8J16 FRT^{2A}/TM6B* or ♂*9E6 FRT^{2A82B}/TM6B*. After three days flies were transferred to a new vial. The original vial was then heat shocked at 37°C for one hour to induce homologous recombination at the FRT sequences. Four days later, as third instar larvae began to crawl, a second heat shock at 37°C for one hour was performed to induce the expression of GFP. Vials were set

for one hour at room temperature before harvesting third instar larvae for dissection. Primary dissection was performed in 1X Phosphate Buffered Saline (PBS, see Appendix C). Primary dissection involved bisecting and inverting the anterior half of the larvae, exposing internal organs and structures to the outside and allowing antibodies access to tissues for staining. Inverted larvae were then fixed in 1X PBS with 4% formaldehyde for 20 minutes at room temperature. Following fixation, larvae were rinsed four times and washed four times for seven minutes each in PBS with 0.1% TritonX-100 (PBT, see Appendix C) at room temperature. A 30-minute block in PBT with 5% Normal Horse Serum (PBTN, see Appendix C) at room temperature followed the washes. Larvae were then incubated in primary antibody diluted in PBTN on a rocker for two hours at room temperature or overnight at 4°C. Antibodies used were against Wg signaling morphogen, targets of Wg and Hh signaling, as well as various compartment makers along the pathway towards the lysosome (see Appendix A). Following primary incubation larvae were rinsed and washed four times each in PBT and incubated in secondary antibody in PBTN for one hour at room temperature. Unless otherwise indicated, secondary antibody staining was performed using Alexa Fluors® from Molecular Probes at a dilution of 1:500 (see Appendix A). Larvae were rinsed and washed four more times each. Finally, secondary dissection, which involved the removal of only the wing imaginal discs from the dissected larvae, was performed in PBT. Dissected wing discs were mounted on a microscope slide in a 70% glycerol-PBS, covered with a 2μm Fisherbrand® Microscope Cover Glass, and sealed with green nail polish. Discs were then visualized under the confocal microscope for mutant phenotypes and images were captured using and Zeiss LSM 780 confocal microscope with Zen software.

2.4 Embryonic Germline Clones

In addition to looking in wing imaginal discs, signaling was also examined in embryos. The female sterile FLP technique was utilized to create females that produce 8J16 germline clone eggs that were fertilized by males that harbor 8J16, 9E6, or $atg18^{KG03090}$ ($atg18^{P}$) mutations, a P-element insertion in the 5' untranslated region (UTR) of *atg18* (Roseman et al., 1995). These same germline clone embryos were used for cuticle preparations performed to confirm 8J16 and 9E6 are, in fact, alleles of *atg18* as well as for the initial embryonic screen that identified 8J16 and 9E6 as mutants that affect Wg or Hh signaling (see Figure 1).

2.4.1 Generating Embryonic Germline Clones

During *Drosophila* oogenesis, approximately 30% of the 13,000 genes of the *Drosophila* genome are deposited into the developing oocyte. The presence of this maternal load of wild type gene products into an otherwise mutant embryo allows this embryo to survive to later stages of development, often masking the effects of a mutation early in development. In order to circumvent this issue of the maternal load and to analyze fully mutant embryos, heat shock driven site-specific FLP recombination with a dominant female sterile ovo^{D1} mutation was employed to generate embryonic germline clones. One copy of ovo^{D1} causes female sterility by blocking early oogenesis. Recombination after G2 between nonsister chromatids results in three types of recombinant products. The only embryos that complete oogenesis are those lacking ovo^{D1} and carrying two copies of the mutation (Figure 11) (Selva & Stronach, 2007).

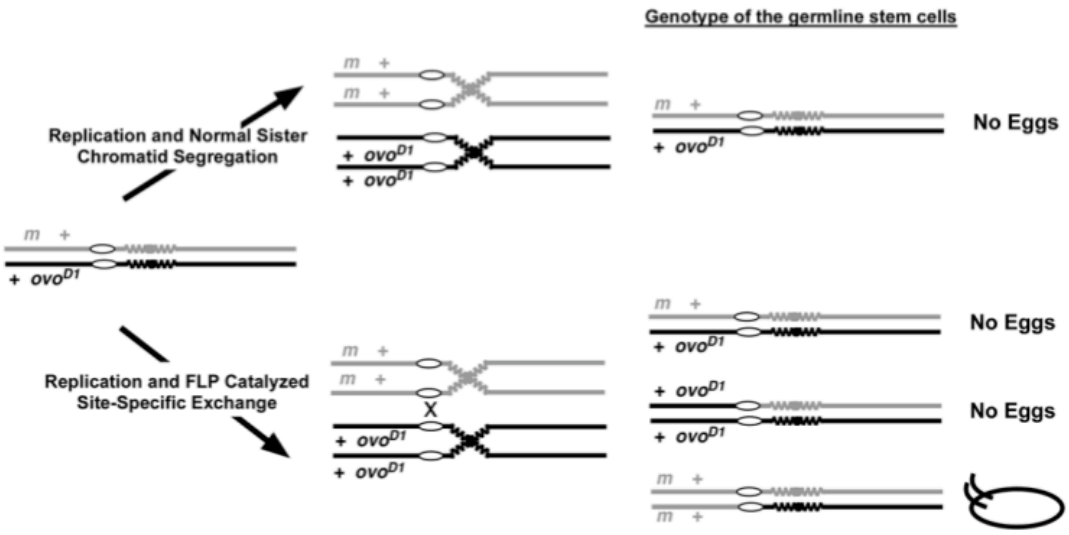

Figure 11. **FLP recombination system used to produce embryonic germline clones.** Recombination between nonsister chromatids results only in embryos carrying the mutation (Figure adapted from Selva & Stronach, 2007).

When fertilized by heterozygous males, these embryos could be analyzed for the effects of a mutation on early stages of development. Additionally, the paternal rescue effect, which occurs as a result of receiving the wild type copy from the heterozygous father, allowed comparison of these progeny to fully mutant embryos. For analysis of staining of embryos with immunofluorescent antibodies (see section 2.5.4 and Appendix A), paternal rescue embryos were identified by the presence of a twist-GFP marker. In cuticle preparations, paternal rescue embryos were visually identified by a less severe phenotype (see results Figure 18). Appendix D depicts the series of crosses used to generate *atg18* germline clone embryos.

2.4.2 Embryo Collection Protocol

The protocol followed for preparing embryo collection plates made enough for about 60- 30 mm Petri dishes. 750 mL distilled water was combined with 25 grams of agar and autoclaved in a two liter flask for a 20 minute liquid sterilization cycle. While the agar was being autoclaved, 25 grams sucrose was dissolved in 250 mL apple juice. This solution was added to the agar immediately after it was removed from the autoclave. The solution was allowed to cool to approximately 60°C, at which time 1.5 grams of Tegosept antifungal was dissolved in 10 mL of 100% ethanol. Once agar was cool the Tegosept solution was added. Plates were then filled about half way, flamed briefly with a Bunsen burner, allowed to solidify, and stored at 4°. Crosses were set up and kept in collection containers on agar plates. Finely ground yeast and water were combined to make a yeast paste food supply, which was added to each plate using a syringe.

2.4.3 Cuticle Preparation

In order to confirm that $atg18^{8J16}$, $atg18^{9E6}$ and $atg18^{P}$ were allelic, 8J16 germline clones eggs fertilized by 8J16, 9E6 or $atg18^{P}$ males were compared to examine differences in embryonic cuticle phenotypes. Wild type controls were also performed using w^{1118} flies. Embryos were collected after 24 to 48 hours and set at room temperature for 24 hours. At this time plates were cleared and embryos were collected. Collections were performed by cleaning the plate of any debris, adding distilled water, and gently scraping embryos from the plate. Embryos were then collected by filtering through thin mesh. Embryos were dechorionated with a 50% bleach solution for five minutes. Following dechorionation, embryos were rinsed thoroughly with distilled water and placed into a microcentrifuge tube containing a 1:1

heptane:methanol solution. Embryos were then vortexed for one minute to devitillinize the embryos. This step was not performed in initial characterization of 8J16 and 9E6 embryos (Figure 1). Embryos that had not cracked out after vortexing were removed along with the upper heptane layer. Embryos were washed three times with methanol and then the methanol was removed. 60 µl Hoyer's mounting media (see Appendix C) mount solution was added to devitillinized embryos and allowed to equilibrate for ten minutes before being pipetted onto glass microscope slides and covered with a cover slip. Slides were left overnight on an incubator at 55°C, allowing the Hoyer's media to break down tissues inside the cuticle. The following day slides were allowed to cool, cuticles were visualized using dark field microscopy on a Zeiss auxiophot, images were captured, and embryo phenotypes were scored.

2.4.4 General Antibody Staining Protocol for Whole Mount Embryos

Flies used for antibody staining were 8J16 germline clone virgin females crossed to 8J16, 9E6, and $atg18^{P}$ males. The goal of these experiments was to examine signaling within embryos in order to further characterize the effect of the mutants on signaling. GFP expression was utilized in this experiment, with positive GFP marking the paternal chromosome that carries a wild type copy *atg18*. Non-paternal rescue embryos were distinguished by lack of GFP expression. Control experiments were also conducted on wild type flies of the genotype w^{1118}. Flies were crossed and kept in collection containers on agar plates with yeast paste, and embryos were collected every eight or 16 hours. Embryos were dechorionated with a 50% bleach solution for five minutes, removing the outer membrane. Embryos were then rinsed thoroughly with distilled water and placed in a microcentrifuge tube containing 1:1 heptane:PEM-FA (see Appendix C), which was made just before use. Embryos

were then placed on a shaker on high for 20 minutes for heptane to disrupt the inner membrane and allow the fixation. The PEM-FA was then removed (aqueous, bottom layer) using a transfer glass pipet and an equal volume of methanol was added. At this stage there should still be two distinct layers. If two layers were not visible, more heptane was added. Embryos were vortexed for one minute to remove the inner, hydrophobic vitellin membrane, causing the devitellinized embryos to sink to the bottom of the tube. The embryos that were not devitellinized remained at the interface and were removed along with the heptane layer (top). Devitellinized embyos were then washed three times with methanol. At this point embryos were stored in methanol at -20°C (good for one year or longer). For immediate use or for embryos stored in methanol, embryos were rinsed four times then washed four times for seven minutes each in PBT. Embryos were blocked in PBTN for 30 minutes at room temperature. Primary incubation was performed in PBTN with various antibodies at antibody dependent dilutions for two hours at room temperature or overnight at 4°C (see Appendix A). Embryos were again rinsed and washed in PBT and incubated in secondary antibody in PBTN for one hour (see Appendix A). Rinses and washes were repeated one final time before removing as much buffer as possible, leaving only embryos. 25 µl of 70% glycerol was added to the embryos, which were allowed to equilibrate overnight at 4°C. When all of the embryos had settled to the bottom they were mounted on a slide, covered, and sealed with green nail polish. Embryos were then visualized on the confocal microscope and images were captured.

2.5 Sequencing the 8J16 and 9E6 Mutations

Following phenotypic characterization of the mutants, experiments were directed at determining the molecular basis of the 8J16 and 9E6 mutations. This was

accomplished through sequencing genomic DNA, which involved preparing genomic DNA, using designed primers and the polymerase chain reaction (PCR) to amplify the gene region, purifying the PCR products, and sending products for sequencing. The mutant flies used for sequencing were transheterozygotes of the genotype ♀8J16 FRT^{2A}/TM6B or ♀9E6 FRT^{2A82B}/TM6B. These flies contained both a mutant and a wild type balancer chromosome, which was used to distinguish the mutants in the analysis of sequencing results. Primers were designed to cover the *atg18* gene region for amplification and sequencing of this gene. The primer names are number designations referring to the location of the primer in *atg18* genomic DNA (see Appendix B). Sequencing results were analyzed using Sequencher, a Gene Codes Corporation DNA analysis software.

2.5.1 Isolation of Genomic DNA

In order to sequence *atg18* in the mutants, the first step was to isolate genomic DNA from both 8J16 and 9E6 mutant flies. FlyBase expression data was used to determine the best tissue from which to extract genomic DNA, and adult male flies aged day three to seven were chosen due to a high expression of *atg18* at this stage. Thirty flies were collected and placed in a blue microcentrifuge tube on ice. 200 µl of Fly Genomic DNA Solution A (see Appendix C) was added and flies were homogenized with a plastic pestle. Homogenate was then incubated for 30 minutes at 70°C. 28 µl of 8M KOAc was then mixed in and followed by a 30-minute incubation on ice. The sample was pelleted at 14,000 revolutions per minute (rpm) at 4°C for 15 minutes and supernatant was transferred into a fresh microcentrifuge tube. 15 µl of resuspended STRATACLEAN resin slurry was added to the supernatant and mixed on a rocker at room temperature for three minutes. Resin was pelleted at 14,000 rpm for

one minute at 4°C and supernatant was again transferred into a clean microcentrifuge tube. DNA was then precipitated by adding 114 µl of isopropanol at room temperature, mixing the sample, and centrifuging at 15,000 rpm for 5 minutes at room temperature. After removal of isopropanol, the pellet was washed with 500 µl of cold 70% ethanol. Ethanol was then removed and the pellet was allowed to dry completely. Finally, the pellet was resuspended in 100 µl 1X TE. This procedure was followed by a phenol:chloroform extraction. 100 µl of a 1:1 phenol:chloroform solution was added to the reconstituted DNA, vortexed for two minutes and centrifuged at 15,000 rpm for one minute. Next, the aqueous extraction was performed in which the resulting top phase of this spin was removed and transferred to a clean microcentrifuge tube. This was followed by a back extraction in which 50 µl 1X TE was added to the remaining bottom phase, vortexed for one minute, and spun for one minute at 15,000 rpm. To this, the previously extracted top phase was added along with 15 µl 3M NaOAc and 300 µl 100% ethanol. The sample was then cooled at -80°C for 30 minutes. To complete the extraction the sample was pelleted by centrifuging at 4°C for ten minutes at 14,000 rpm and the top aqueous layer was removed. The pellet was washed with 500 µl cold 70% ethanol, dried completely, resuspended in 30 µl 1X TE, and stored at -20°C for later use.

2.5.2 PCR

The protocol followed and products used for PCR were from Invitrogen. Generally, 1 µg of DNA was used as a template. Each reaction was set up on ice in sterile PCR tubes containing 1 µg DNA template, 5 µM forward primer, 5 µM reverse primer, 10X reaction buffer, 200 µM dNTPs, and 1.25 units Platinum® *Taq* DNA Polymerase (5 units/µl). Typically, 25 µl reactions were performed, using distilled

water to bring the reactions up to the appropriate volume. Often a master mix was made containing the reaction buffer, the dNTPs, and the DNA polymerase, which was always added last. Once all reactions were set up, they were immediately placed into a pre-programmed thermocycler and run as follows: 94°C hot start for one minute to ensure DNA is fully denatured initially, followed by 30 cycles of 30 seconds at 94°C for DNA denaturation, one minute at the appropriate annealing temperature for the included primers, and a one minute per kilobase extension at 72°C. Products were then stored at 4°C.

2.5.3 DNA Isolation for Sequencing

After PCR amplification, protocols were employed in order to prepare DNA to be sent for sequencing. The DNA Clean & Concentrator™-5 Protocol from ZYMO Research Corporation was used for certain samples. This uses a Zymo-Spin™ column for the elution of highly concentrated, purified DNA suitable for PCR and DNA sequencing. Extraction of samples directly from the agarose gel was performed using NucleoSpin® Extract II's protocol for DNA Extraction from Agarose Gel. For remaining samples, PCR products were purified using NucleoSpin® Extract II's protocol for PCR Cleanup. Once purified DNA product samples were collected, nanodrop quantification was performed in order to determine DNA concentration. Samples were sent for sequencing at a concentration of 2 ng/µL in Eppendorf PCR tubes.

2.6 Agarose Gel Electrophoresis

Conditions used for agarose gel electrophoresis varied widely depending on the experiment being conducted. For general visualization, a standard Genetic

Analysis Grade Agarose from Fisher Scientific was used. For products to be purified, a higher quality SeaKem® GTG® Agarose from Lonza was used. Agarose HR (High Resolution) form Denville Scientific, Inc. was used for gel electrophoresis of products 50-1000 base pairs in length. For a higher quality analysis of nucleic acids less than one kilobase in length, NuSieve® 3:1 Agarose from Lonza was used. The concentration of agarose used for gels was between one and three percent with the higher percentage gels being used for smaller products as well as for a more distinct separation of bands. Smaller gels required 25 µl total, while a larger gel required 40 µl. To make the gel, the specified amount of agarose was measured and placed in a flask. To this, the appropriate amount of 1X TAE (see Appendix C) was added. The mixture was microwaved on 50% power in 30-second intervals, avoiding bubbling over, until all agarose powder was dissolved. The mixture was allowed to cool just enough so that it would not melt the mold, but not so long that the agarose began to solidify. Once cooled, the agarose was poured into the mold for the appropriate number of wells needed and allowed to solidify. When the gel was completely solidified, it was transferred the electrophoresis apparatus. While the gel was solidifying, samples were prepared by adding 6X Gel Loading Dye Blue (New England BioLabs® Inc.) to each sample for a final concentration of 1X. When samples were ready to be loaded, the apparatus was filled with running buffer (1X TAE) and samples were loaded into their designated wells. In general, gels were run at 100V for 30 minutes, but the length of time varied with the concentration of the gel, with a longer run time being employed for higher percentage gels. For greater band separation, gels were run for longer at only 50V. Upon completion, the gel was transferred to an ethidium bromide-water solution to stain the gel (see Appendix C).

This allowed for visualization of the DNA under UV light due to ethidium bromide's ability to intercalate into DNA bases. Typically, staining was performed for ten minutes and followed by a 15 minute de-stain in distilled water. At this point gels were visualized under UV light and images were captured.

2.7 RNA Isolation Protocol

All RNA isolations were performed using the Total RNA Isolation kit and user manual guidelines from Macherey-Nagel's NucleoSpin® RNA II. During isolation, all conditions were optimized for RNA conditions, ensuring everything was kept RNase free. Each RNA isolation was from approximately 80 pupae (~100 mg sample). Pupae were collected and stored at -80°C. RNA extraction was performed following the kit protocol. Final RNA quality and quantity were measured using a Nanodrop. Pure RNA threshold was determined to be samples with a 260/280 reading of around two. Quantity of RNA was measured in units of ng/µl.

2.8 One-Step Reverse Transcription-PCR (RT-PCR)

For analysis of RNA samples, reverse transcription to make cDNA and PCR were performed simultaneously. The protocol followed and kit used was Invitrogen's SuperScript® II One-Step RT-PCR with Platinum® *Taq* DNA Polymerase. Samples were then run on gels following the procedure described in section 2.5.

2.9 Quantitative PCR (qPCR)

For all qPCR experiments, extracted total RNA was used as a template for first strand cDNA synthesis using Invitrogen's SuperScript™ III Reverse Transcriptase kit. For all reactions, 1 µg RNA and oligo$(dT)_{18}$ primers were used. The protocol was followed under RNase free, sterile conditions. After cDNA synthesis, qPCR was

performed following the protocol by Qiagen© for SYBR Green qPCR. Experiments were set up using primers specifically designed for qPCR, which have a product size of less than 100 base pairs. Additionally, one primer was designed to span the exon-exon junction to ensure only processed RNA was being examined (see Appendix B). Two mixes were made, one containing primers and the SYBR Green master mix and the other containing a mix of cDNA and water. These were added to the appropriate wells of a 96-well PCR plate, mixed, and centrifuged. PCR was performed with a 95°C hot start for 15 minutes followed by 40 cycles of 15 seconds at 94°C (denaturation), 30 seconds at 55°C (annealing), and 30 seconds at 72°C (extension) using the ABI 7000. Thresholds for cycle count were set by the program used for the PCR run. Data was exported and analyzed in Excel.

Chapter 3

RESULTS

3.1 Characterization of Wing Imaginal Discs Indicate a Wg Gain-of-Function Phenotype

Characterization of 8J16 and 9E6 was performed for a wide range of markers within the wing disc. Antibodies were used to stain for Wg, short- and long-range targets of Wg, targets of Hh, and endocytic vesicles along the pathway towards the lysosome (see Appendix A). Wg and Hh short range signaling was not altered in 8J16 or 9E6 mutant tissues (data not shown). Contrary to my hypothesis, there was an indication of a slight Wg gain of function phenotype, as shown by the long-range target, Distalless (Dll, Figure 12). Extensive experimentation showed no change in endocytic vesicles (data not shown).

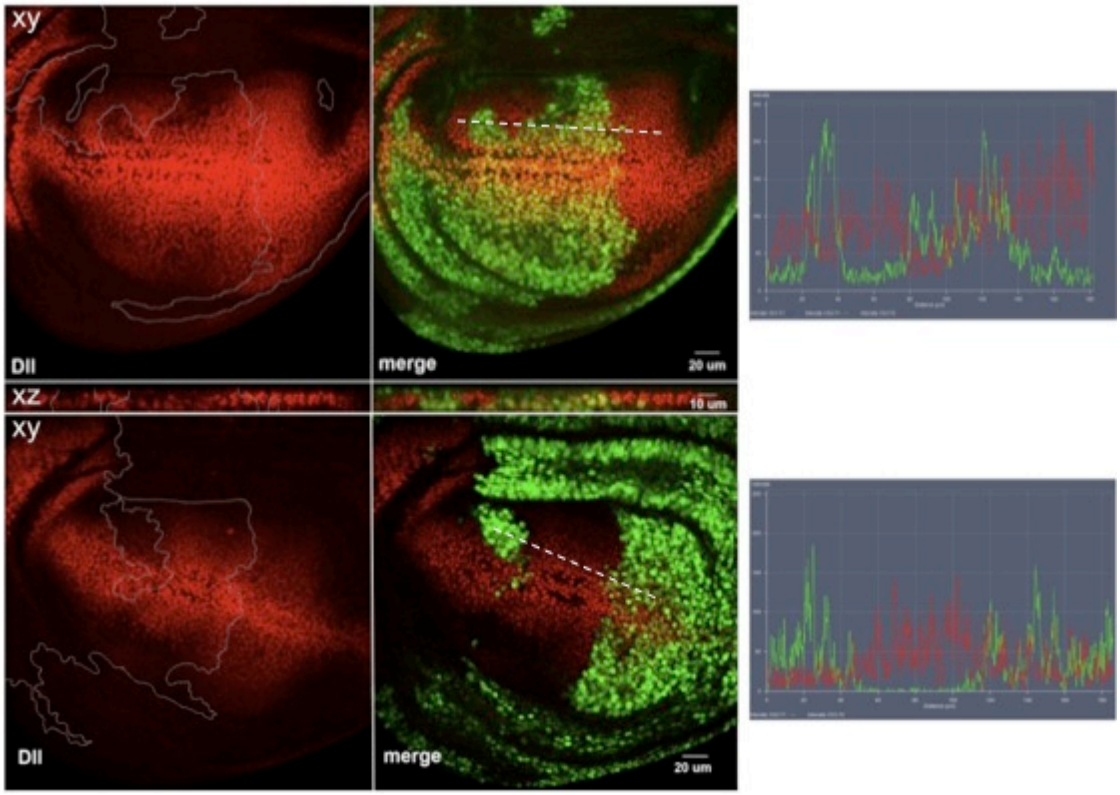

Figure 12. **Mosaic analysis of *Drosophila* wing imaginal discs shows a slight Wg gain of function phenotype as indicated by the expansion of the long-range target, Distalless (Dll, red).** Homozygous mutant tissue is marked by the absence of GFP, and white lines on the images to the left outline these clones. 8J16 (top) and 9E6 (bottom) mutant tissue show the expansion and increased intensity of Dll, indicating enhanced long-range Wg signaling. Intensity plots, pictured on the right, confirmed this phenotype. Signaling intensity was measured along dashed white lines pictured in merge image. All discs are oriented dorsal up and anterior left.

3.2 Wg and Central Nervous System (CNS) Defects in Embryos

Analysis of embryonic germline clones for several different markers using antibodies revealed two major findings. First, both 8J16 and 9E6 show a loss of Wg at stage 9 (Figure 13). Mutation in *atg18* also causes a severe CNS defect that is not

strictly the result of loss of Wg signal transduction. The CNS phenotype was analyzed by staining markers of CNS differentiation and development (Figure 14).

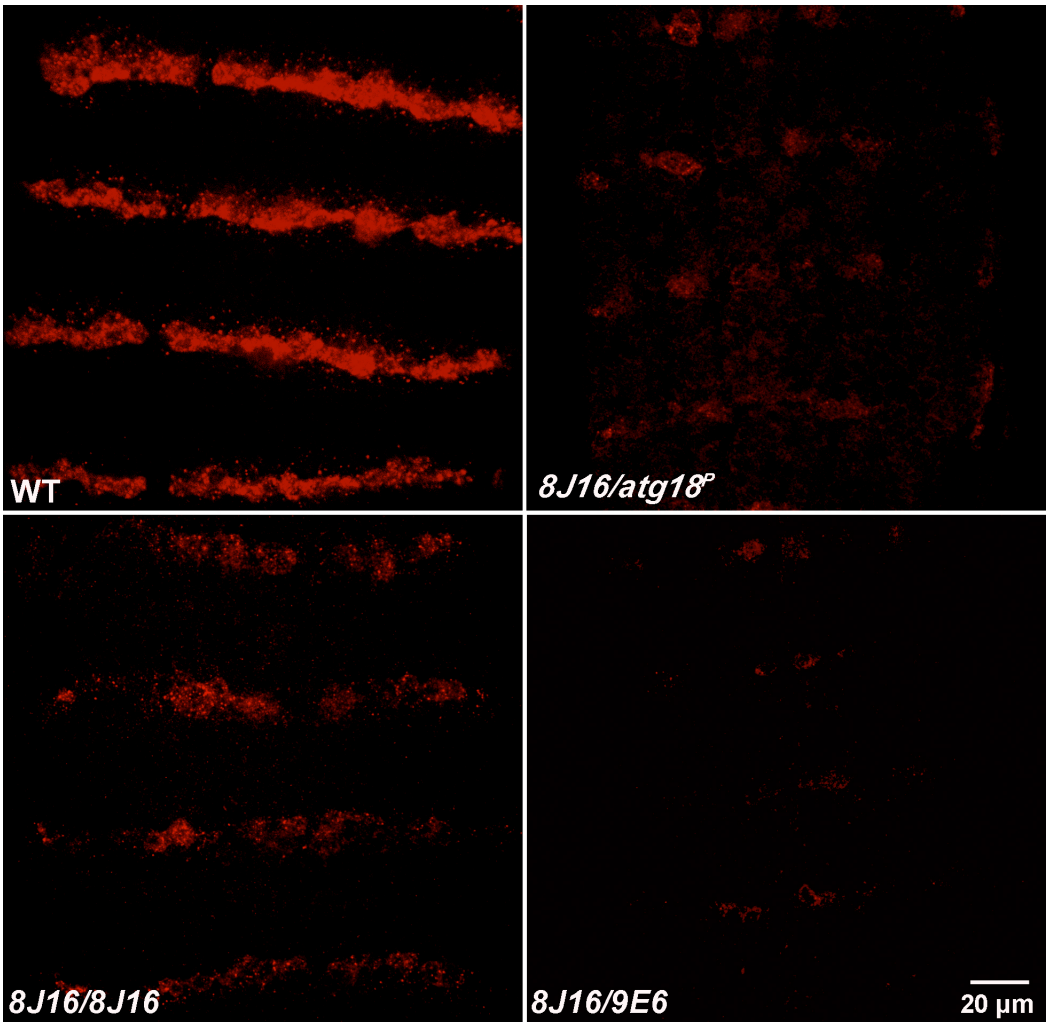

Figure 13. **8J16 and 9E6 show a loss of Wg expression at embryonic stage 9 that may be the cause of observed segmentation defects.** Germline clone embryos were collected and stained with Wg (red). A twist-GFP balancer staining (not shown) was used to distinguish mutants (GFP negative) from paternal rescue embryos (GFP positive, also not shown). Staining shows fading of Wg expression during embryonic stage 9. Loss of Wg during embryogenesis is predicted to yield characteristic patterning defects observed in embryonic cuticles (Figure 1).

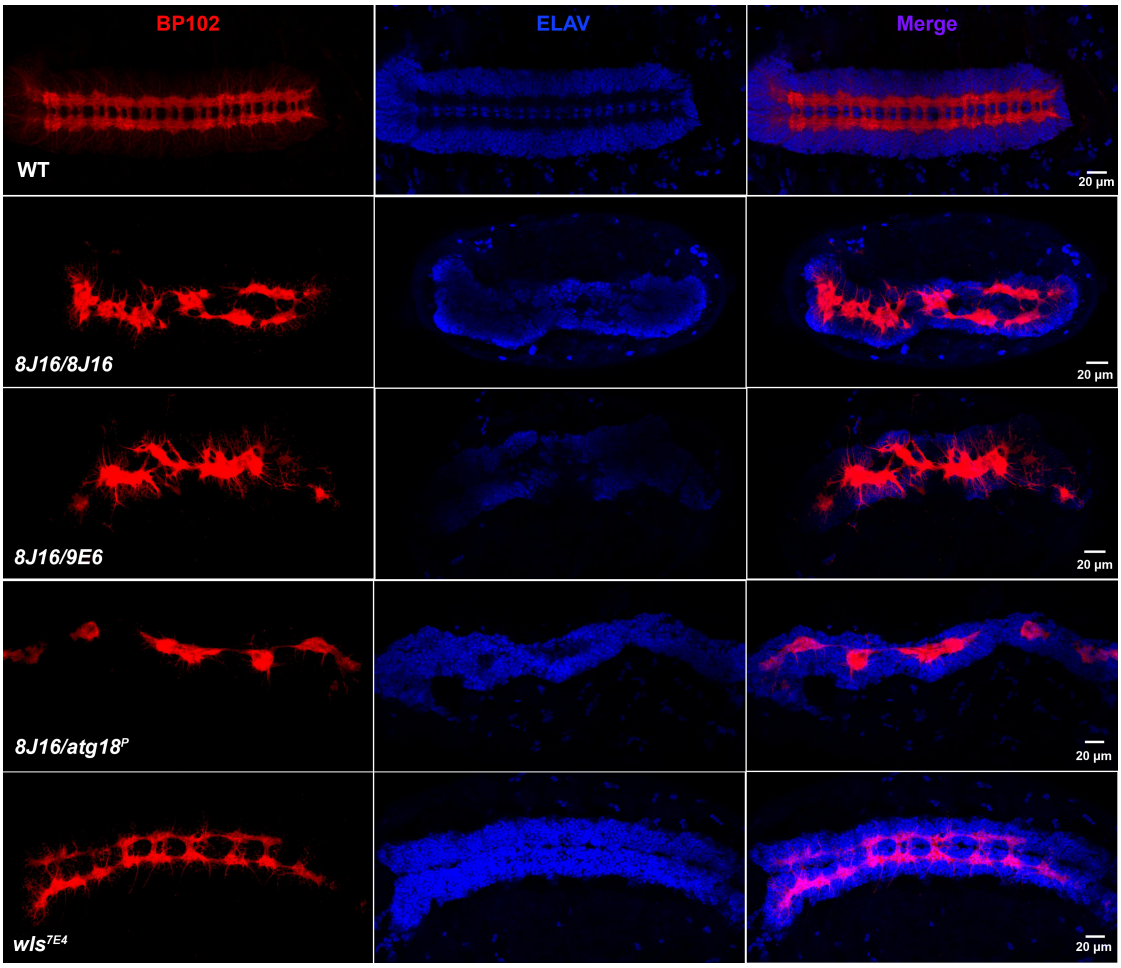

Figure 14. **8J16 and 9E6 germline clone mutants show a phenotype indicative of severe CNS defects as compared to wild type embryos.** Embryos were stained for BP102 (red), a neuronal marker of the CNS, and ELAV (blue), a pan-neuronal marker. The same defects were seen in *atg18*^{P} embryos. *atg18* mutant phenotypes are much more severe than *wls*^{7E4,} a mutation that blocks Wg signaling, suggesting *atg18* mutations have more pleiotropic effects during embryogenesis.

3.3 8J16 and 9E6 are Intronic Point Mutations

The result of sequencing *atg18* in the mutants was the discovery of independent, intronic point mutations in both 8J16 and 9E6. The sequencing results for *atg18* were examined, and these point mutations were discovered by the presence

of two peaks, indicating the change in the mutant. 8J16 is a change from a G to an A within the third intron at nucleotide 1761, the change most predicted with EMS mutagenesis. 9E6 is G to a T change at nucleotide 2611 (Figure 15).

Figure 15. ***atg18* gene region showing 8J16 and 9E6 mutations are point mutations within introns.** The 8J16 mutation is a change within the third intron from a G to an A at nucleotide 1761. The 9E6 mutation is a change from a G to a T at nucleotide 2611 in the fourth intron.

3.4 Splicing is Not Affected by 8J16/9E6 Intronic Point Mutations

Following the discovery that 8J16 and 9E6 are intronic point mutations, I hypothesized these intronic point mutations affected splicing of the mRNA transcript, leading to the observed mutant phenotypes. With this hypothesis, differences in the RNA product should be observed when primers specifically designed to span introns were used to make and amplify *atg18* cDNA (see Appendix B, Figure 16). Results of this splicing analysis did not indicate a change in splicing, as shown by product sizes consistent with those seen in wild type flies (Figure 17). The external control for splicing experiments was Actin5C.

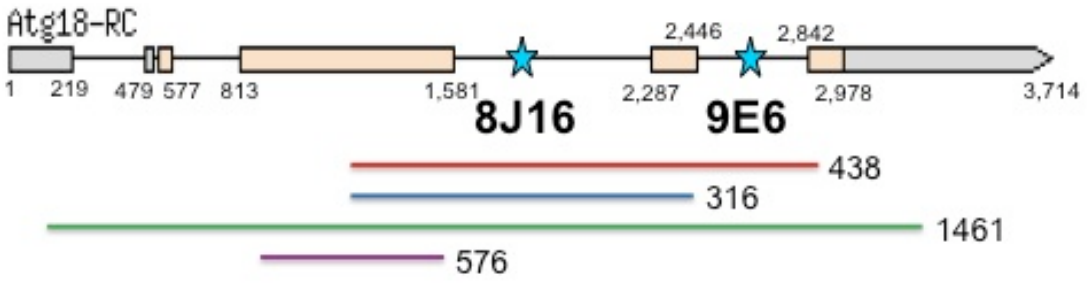

Figure 16. **Primers used to examine splicing of *atg18* were designed to span introns.** Colored bars correspond to primer pairs indicated on the gel image showing the results of examining splicing (Figure 17). Numbers listed to the right of each bar are the expected fragment size for each primer pair when properly spliced. The purple bar represents an internal control primer pair, located within the first major exon, that is not predicted to be affected by the 8J16 or 9E6 mutation.

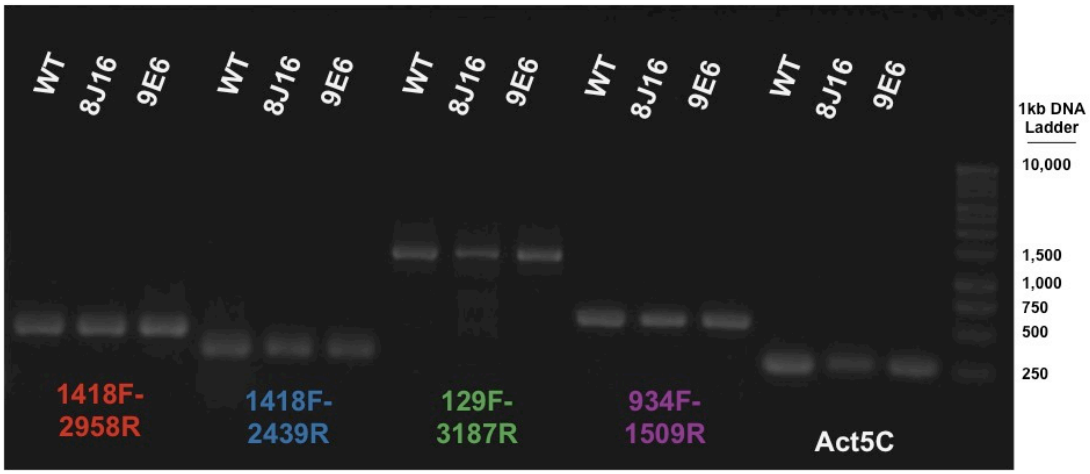

Figure 17. **RT-PCR of 8J16 and 9E6 total RNA shows splicing is not affected by the mutations.** A 1kb DNA ladder was used to indicate fragment sizes (key listed on the right). In all cases spliced product sizes are the same in wild type and mutant flies and are of the predicted length indicated in Figure 16. All samples show a strong signal for the internal control, 934F-1509R, indicating *atg18* RNA in WT and mutants is present at comparable levels. Absence of unspliced product in Act5C, the actin control, indicates a clean RNA isolation.

3.5 *atg18^{8J16}, atg18^{9E6}, and atg18^{P}* are Allelic

Cuticle preparations of embryonic germline clones generated via the dominant female sterile Flp technique for both mutants were compared to that of *atg18^{P}* in order to confirm that 8J16 and 9E6 were, in fact, alleles of *atg18*. The same phenotype was observed in all three, providing sufficient evidence that the mutants are, in fact, alleles of *atg18* (Figure 18).

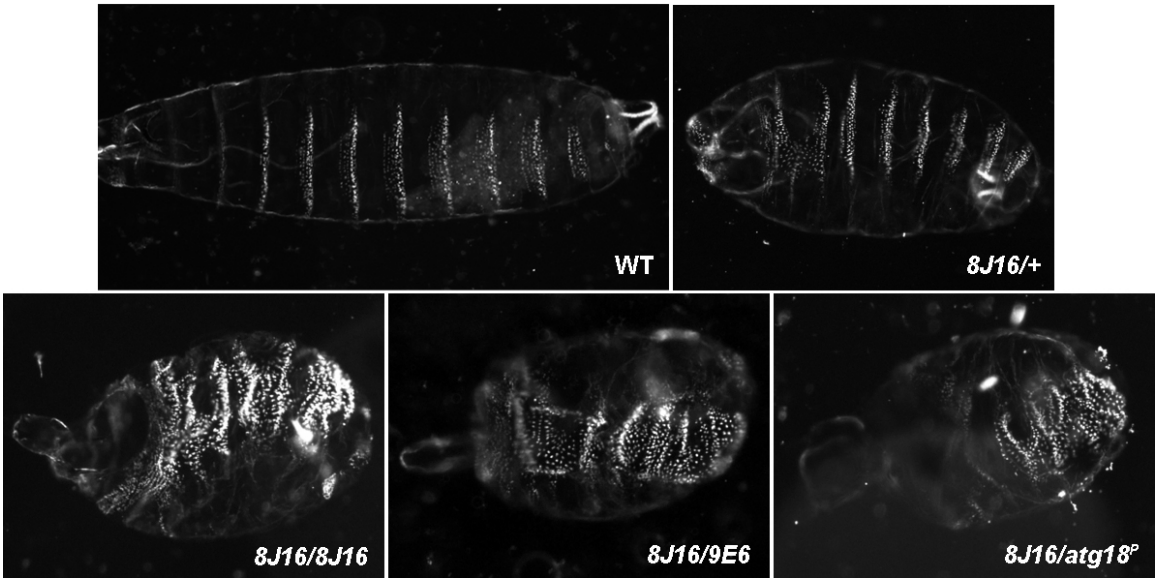

Figure 18. **Cuticle images of germline clone embryos for *atg18^{8J16}/atg18^{8J16}*, *atg18^{8J16}/ atg18^{9E6}*, and *atg18^{8J16}/ atg18^{P}* confirmed all three are allelic.** Each displays the same 'lawn of denticles' phenotype and head defect typical of Wg/Hh signaling loss in the embryo (see Figure 1). Wild type and paternal rescue embryos are included for comparison (top left and top right).

3.6 8J16/9E6 are Rescued at an Elevated Temperature

Another surprising observation made while working with 8J16 and 9E6 was the discovery of a severe temperature sensitivity in the mutants (Table 1). 8J16 and

9E6 show complete rescue at 29°C to pupal stages of development as compared to room temperature (RT, approximately 26°C). Survival rates were greatly impaired at 18°C (data not shown). This same case is not seen, however, in *atg18*^{P} (Table 1).

Table 1. **8J16 and 9E6 show complete rescue at 29°C.** When crossed with flies deficient for the *atg18* gene region, the expectation is that 33% of the pupal offspring will be of the genotype mutant/null, marked by the absence of the tubby marker, TM6B. This number is greatly reduced in 8J16 and 9E6 at room temperature (~26°C) but rescued at the elevated temperature, 29°C. The same observation is not made with *atg18*^{P}.

Cross	RT (~26°C)	% Tb^+	29°C	% Tb^+
♀ $atg18^P$/TM6B,Tb x ♂ED4408/TM6B,Tb	52 Tb^+ 101 Tb^-	34.0%	67 Tb^+ 158 Tb^-	29.8%
♀ 8J16/TM6B,Tb x ♂ED4408/TM6B,Tb	14 Tb^+ 112 Tb^-	11.1%	82 Tb^+ 127 Tb^-	39.2%
♀ 9E6/TM6B,Tb x ♂ED4408/TM6B,Tb	26 Tb^+ 94 Tb^-	21.7%	46 Tb^+ 84 Tb^-	35.4%

3.7 qPCR Shows a Decreased Expression Level at an Elevated Temperature

qPCR was performed in order to examine expression levels of *atg18* in the mutants compared to wild type (WT) as well as comparing the two different temperatures. Samples for each experiment were performed in triplicate in order to eliminate the question of any internal variability. Cycle threshold (CT) was set by the pPCR analysis program and was used to compare transcript levels. Amplification was performed in cycles and the CT for product formation was used as an indication of

initial amount of transcript present. A higher CT indicates fewer transcripts were present in the sample because more cycles were required for detection of the product. The product levels were measured by fluorescence of SYBR Green. Using these CT levels, analysis of qPCR for each sample required calculating a delta CT (δCT) and a delta delta CT (δδCT). δCT was calculated as a means of normalizing the experiment by comparing *atg18* transcript levels to actin. δδCT was calculated by comparing transcript levels of the mutants to WT or transcript levels at RT and 29°C. All results shown are of the primer pair that lies on the exon-exon junction (160F-232R), ensuring only processed RNA is present. Experiments were repeated five times, with the first two (royal blue and red) consisting of only WT samples. The key in Figure 19 applies to all qPCR graphs shown. The first set of data shown in Figure 19 is a chart comparing *atg18* transcript levels of the mutant to that of WT samples, all at room temperature. In all three *atg18* mutants, findings show a reduction of transcript levels compared to WT.

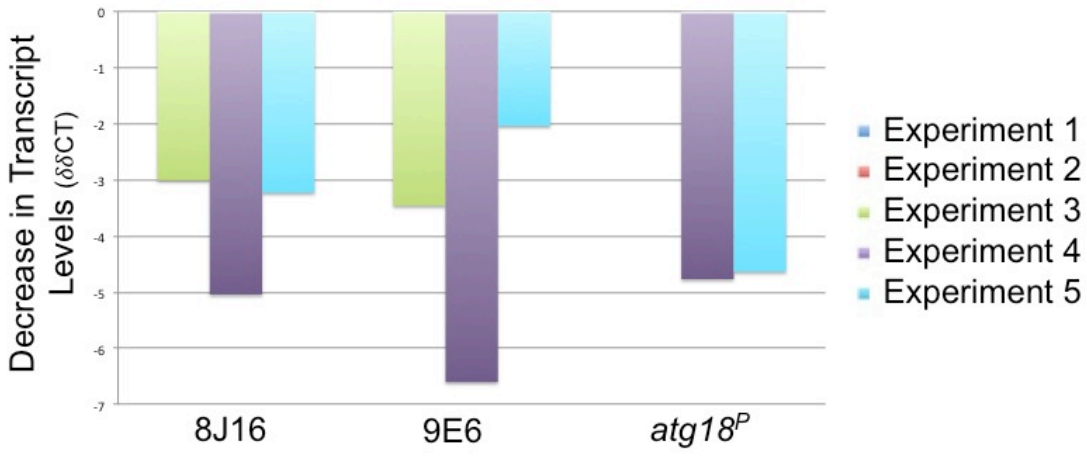

Figure 19. **qPCR analysis of transcript levels in *atg18* mutants shows a reduction of *atg18* compared to WT.**

The second set of data analyzed examined the affect of the temperature change on *atg18* transcript levels. First, levels were examined in WT. Figure 20 is a graph that shows a reduction of transcript levels at 29°C compared to room temperature. This was found to be the case in four out of five experiments. The slight increase found in the fifth experiment will be examined in future experiments directed at addressing variability within these qPCR experiments.

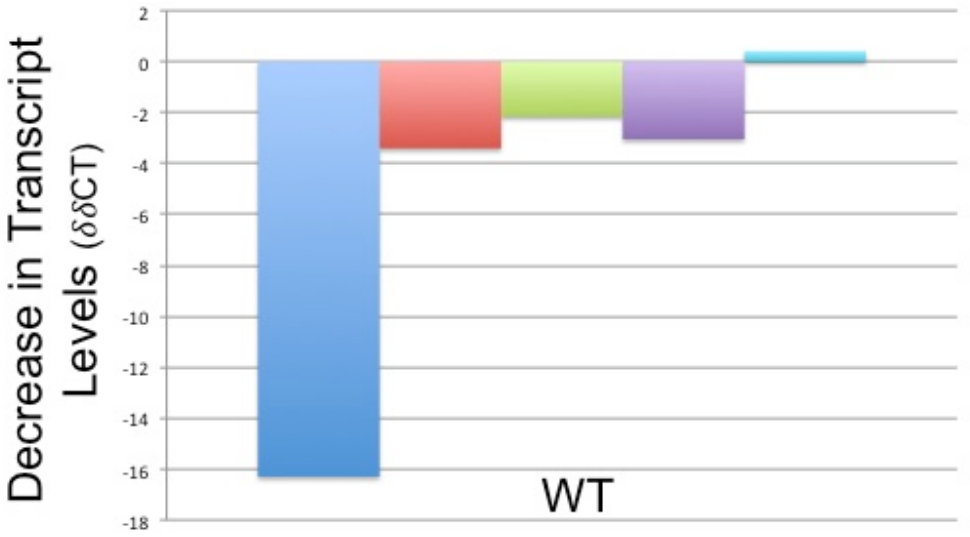

Figure 20. **qPCR shows a reduction of *atg18* transcript levels in WT at the elevated temperature, 29°C, in four out of five experiments.**

Finally, *atg18* expression levels were examined in the mutants, comparing *atg18* mutants to WT at the two different temperatures. Results show an increase in transcript levels at 29°C in the mutants when compared to WT (Figure 21). Again, future experiments are required to address variability seen in 9E6 and $atg18^{P}$.

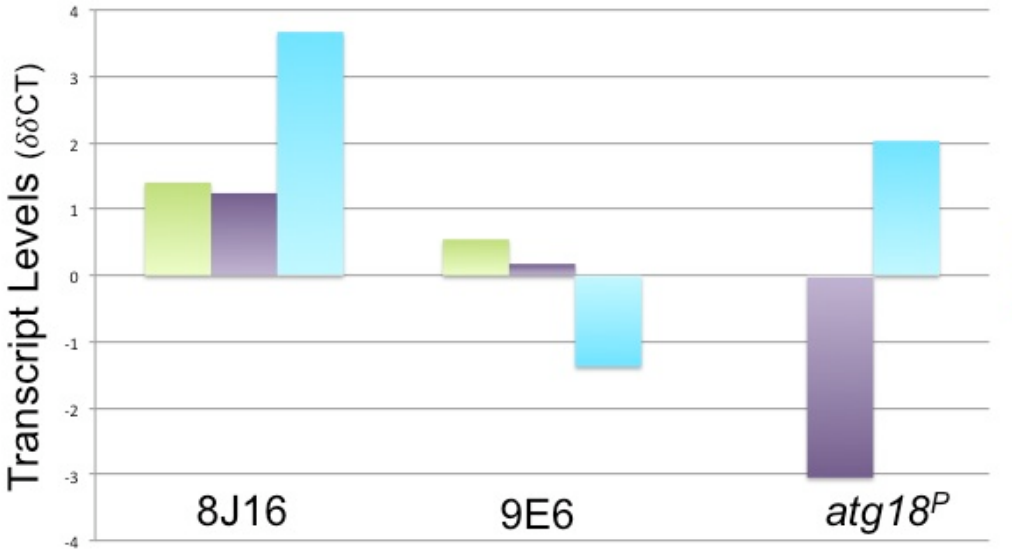

Figure 21. **qPCR shows an increase in transcript levels within the mutants at 29°C as compared to WT.** Future experiments are required to address the variability observed in 9E6 as well as to determine the actual affect of *atg18*^{P} on transcript levels as two different results were obtained in experiments four and five.

3.8 8J16/9E6 Mosaic Under a Non-Heat Shock Promoter May Provide Evidence of a Decrease in Wg Signaling in Mutant Tissue

Upon the discovery of the temperature sensitivity of 8J16 and 9E6, further experiments in the wing disc were conducted to address potential consequences of the heat shock administered in initial characterization required for recombination and GFP expression when creating mosaic clones. Crosses were set up that allowed for the induction of recombination under a GAL4 promoter, eliminating the heat shock as a variable found to have an effect on the mutants (see Appendix D). Discs were stained for Wg in order to determine the effect of the mutants on signaling. Using this non-heat shock system, we find that Wg may be downregulated in mutant tissue (Figure 22). Further experiments are required to confirm this phenotype.

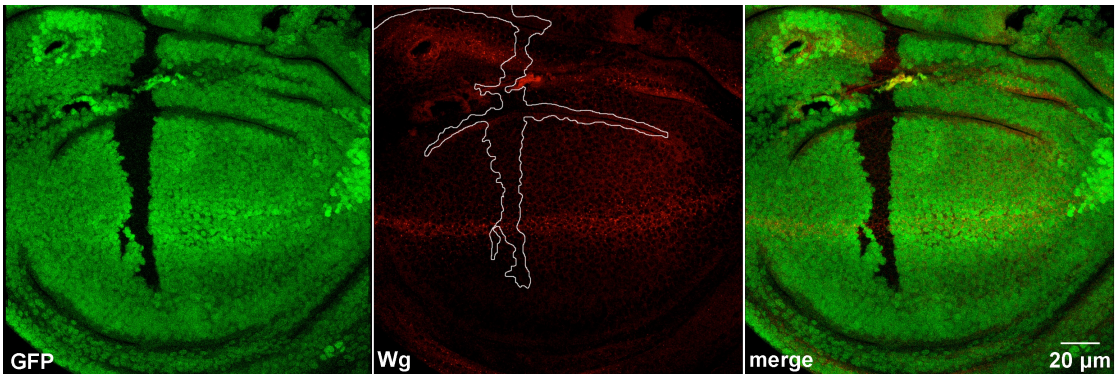

Figure 22. **Using the Gal4 promoter, Wg may show reduced signaling in mutant tissue.** Wg signaling (red) appears to be reduced in 8J16 mutant tissue, outlined in white and marked by the absence of GFP (green). The same observation was made in 9E6 (data not shown).

Chapter 4

DISCUSSION

When work began on this project, my initial hypothesis was that by examining the *Drosophila* wing disc using antibody markers we would observe an increase in the lysosomal compartment at the expense of endosomes and a corresponding decrease in Wg and Hh signaling. Though the vast majority of results were negative, one surprising phenotype was discovered that instead revealed a slight Wg gain of function as indicated by the long-range Wg target, Distalless (Dll). Based on my initial hypothesis we could not come up with an explanation for this phenotype so I then sought to examine the molecular mechanisms behind these mutations. At this point sequencing of the gene was conducted and we found that both 8J16 and 9E6 were intronic point mutations not predicted to affect splicing based on both computer analysis and examination of transcriptional products. Because these mutations are not predicted to affect splicing, one possible explanation is that the mutations affect the promoter region of *atg18*. I did not sequence the promoter, which is something that could be examined in future experiments. In order to determine if the expansion of Dll seen in wing discs was a result of increased signaling in the embryo, I examined germline clone embryos stained for Wg. As expected, however, the loss of Wg expression at stage nine characteristic of segmentation defects was observed. 8J16 and 9E6 were also compared to $atg18^{P}$, which also showed this same loss of Wg signaling in the embryo. The conclusions drawn from this experiment show these mutations do result in a loss of Wg signaling, however this does not explain the expansion of long-range Wg targets in later development. Another observation made

while examining signaling in the embryo was a severe CNS defect in *atg18* mutants. The CNS defects in *atg18* mutants was compared to that of wls^{7E4}, a mutant that blocks Wg signaling. Staining shows that mutations with *atg18* result in more severe CNS defects than a mutation only affecting Wg signaling, suggesting mutations within *atg18* have more pleiotropic effects during embryogenesis. Before continuing with experiments examining *atg18* function, experiments were conducted to confirm 8J16 and 9E6 are in fact alleles of *atg18*. This was confirmed by examining the cuticle phenotype 8J16/9E6 germline clone embryos and comparing them to the $atg18^{P}$. All three show the same 'lawn of denticles' phenotype and head defect typical of Wg/Hh signaling loss in the embryo, and from this we can confirm all three are alleles of *atg18*.

Another surprising finding discovered while working with 8J16 and 9E6 was a severe sensitivity of the mutants to temperature changes. At room temperature mutant survival rates are severely impaired and die before reaching pupal stages of development. When moved to an elevated temperature, 29°C, mutants show complete rescue of pupal viability. From this I hypothesized an increase in *atg18* transcript levels at 29°C, providing an explanation for the recue phenotype evident at the higher temperature. Prior to performing quantitative PCR (qPCR) experiments, I performed RT-PCR on RNA isolated from mutant pupa at room temperature and the elevated temperature, 29°C. Results were not quantitative, yet a more intense band indicating a higher transcript level at the higher temperature led me to pursue the examination of this in a quantitative manner via qPCR. Results from these qPCR experiments have elucidated findings of differences in the transcript levels when comparing the wild type to the mutants and also comparing levels at the differing temperatures. I found a

decrease in *atg18* transcript levels in the mutant in comparison to WT at ~26°C (RT). I also found an average five-fold decrease in expression of *atg18* at the elevated temperature in WT samples. This result may explain the decrease in survival rate observed at room temperature. When comparing mutants to WT, I found an increase in *atg18* expression at the elevated temperature, 29°C, which may account for the rescue phenotype. The rescue may also be due to a reduced requirement for *atg18* at 29°C. As a result of variability among experiments and possible errors during the experimental procedure, qPCR will need to be repeated to obtain statistical significance. Additionally, the information derived from these experiments is only a starting point for the next series of experiments that will set out to explain the molecular mechanism behind this phenotype.

After observing the temperature sensitivity I sought to identify a major issue with the first set of experiments conducted on the wing disc. The first system used required a heat shock, which is now predicted to affect the observed phenotype as a result of this temperature sensitivity. To address this I utilized a non-heat shock recombination to begin the re-examination of the mutant phenotype in the wing disc. Further experiments will be conducted using this GAL-4 promoter to examine additional signaling targets and intracellular compartments within the wing disc. All initial stainings will be repeated in order to determine if my initial hypothesis does in fact stand with support from these experiments. Additionally, in my initial experiments conducted on the wing disc I was not able to directly stain for the lysosomes. Recent experiments by a fellow lab member showed successful staining of the lysosome using the LAMP1 antibody, which will be used in future experiments to examine the effect of the mutations on the lysosomal compartment. Improvements to

the Gal4 non-heat shock recombination system will also be made when we are able to successfully obtain homozygous e22Gal4UASFlp, which will result in a larger number of wing discs containing clones.

At the completion of my work on this project, I have made many discoveries regarding the 8J16 and 9E6 mutations yet there is still much to be done in order to fully elucidate the means by which 8J16 and 9E6 are causing the observed phenotypes at a molecular level. A summary of conclusions drawn from this project regarding the 8J16 and 9E6 mutations is as follows:

1. *atg18*^{8J16}, *atg18*^{9E6}, and *atg18P* are allelic
2. 8J16 and 9E6 do not increase targeting to the lysosome in wing discs. Contrary to my prediction, Wg shows a slight gain of function in mutant tissue, as shown by the expansion of the long-range target, Dll.
3. 8J16 and 9E6 germline clone embryos show the segmentation defect caused by a loss of Wg at stage 9, as well as severe CNS defects.
4. Mutants are rescued at an elevated temperature.
5. qPCR experiments showed *atg18* transcript levels are lower in mutants when compared to WT at 25°C. The expression of *atg18* is also reduced in WT at the elevated temperature, 29°C, compared to RT. Finally, I observed an increase in transcript levels in the mutants at the elevated temperature when compared to WT, which may provide an explanation for the rescue of the mutants at 29°C.
6. Examination of signaling using a non-heat shock recombination system in wing imaginal discs may show a slight decrease in Wg signaling, which may support my initial hypothesis after further experimentation.

REFERENCES

Berry, D. L., & Baehrecke, E. H. (2007). Growth arrest and autophagy are required for salivary gland cell degradation in Drosophila. *Cell, 131*(6), 1137-1148. doi: 10.1016/j.cell.2007.10.048

Clevers, H. (2006). Wnt/beta-catenin signaling in development and disease. [Review]. *Cell, 127*(3), 469-480. doi: 10.1016/j.cell.2006.10.018

Efe, J. A., Botelho, R. J., & Emr, S. D. (2007). Atg18 regulates organelle morphology and Fab1kinase activity independent of its membrane recruitment by pho sphatidylinositol 3,5-bisphosphate. *Molecular Biology of the Cell, 18*(11), 4232-4244. doi: 10.1091/mbc.E07-04-0301

Fernández-Moreno, M. A., Farr, C. L., Kaguni, L. S., & Garesse, R. (2007). Drosophila melanogaster as a model system to study mitochondrial biology. *Methods Mol Biol, 372*, 33-49.

Geissler, K., & Zach, O. (2012). Pathways involved in Drosophila and human cancer development: the Notch, Hedgehog, Wingless, Runt, and Trithorax pathway. [Review]. *Annals of Hematology, 91*(5), 645-669. doi: 10.1007/s00277-012-1435-0

Goodman, R. M., Thombre, S., Firtina, Z., Gray, D., Betts, D., Roebuck, J., . . . Selva, E. M. (2006). Sprinter: a novel transmembrane protein required for Wg secretion and signaling. *Development, 133*(24), 4901-4911. doi: dev.02674 [pii]

Lin, X. (2004). Functions of heparan sulfate proteoglycans in cell signaling during development. D*evelopment, 131(*24), 6009-6021. doi: 131/24/6009 [pii]

Mathews, C. K., & Van Holde, K. E. (1990). Bi*ochemistry.* Redwood City, Calif.: Benjamin/Cummings Pub. Co.

Mizushima, N. (2007). Autophagy: process and function. Ge*nes & Development, 21(2*2), 2861-2873. doi: 10.1101/gad.1599207

Roseman, R. R., Johnson, E. A., Rodesch, C. K., Bjerke, M., Nagoshi, R. N., & Geyer, P. K. (1995). A P element containing suppressor of hairy-wing binding regions has novel properties for mutagenesis in Drosophila melanogaster. Ge*netics, 141(3*), 1061-1074.

Rusten, T. E., Rodahl, L. M. W., Pattni, K., Englund, C., Samakovlis, C., Dove, S., . . . Stenmark, H. (2006). Fab1 phosphatidylinositol 3-phosphate 5-kinase controls trafficking but not silencing of endocytosed receptors. Mo*lecular Biology of the Cell, 17(9*), 3989-4001. doi: 10.1091/mbc.E06-03-0239

Selva, E. M., & Stronach, B. E. (2007). Germline clone analysis for maternally acting Drosophila hedgehog components. Me*thods Mol Biol, 397,* 129-144. doi: 1-59745-516-4:129 [pii]

Taipale, J., & Beachy, P. A. (2001). The Hedgehog and Wnt signaling pathways in cancer. [Article]. Na*ture, 411(6*835), 349-354. doi: 10.1038/35077219

Theodosiou, N. A., & Xu, T. (1998). Use of FLP/FRT system to study Drosophila development. [Article]. Me*thods-a Companion to Methods in Enzymology, 14(4*), 355-365. doi: 10.1006/meth.1998.0591

Appendix A

ANTIBODIES

Several different antibodies were used to stain wing imaginal discs and embryos. All antibodies were stored at 4°C. For additional uses, primary antibodies were stored with sodium azide (NaN_3). Secondary antibodies were all Alexa Fluor® Dyes that allowed marked targets to be visualized at specific excitable wavelengths via fluorescence excitation under a confocal microscope.

Primary Antibody	**Abbreviation**	**Dilution**	**Marker**
Mouse Anti-Wingless	MαWg	1:10	Wingless Signaling Molecule
Rabbit Anti-Golgi	RbαGolgi	1:500	Golgi
Mouse Anti-Patched	MαPtc	1:10	Hedgehog Receptor
Rabbit Anti-Rab5	RbαRab5	1:500	Early Endosome
Mouse Anti-Armadillo	MαArm	1:10	Segment Polarity Gene (Riggleman)
Guinea Pig Anti-Deep Orange	GpαDor	1:500	Late Endosome
Guinea Pig Anti-HRS	GpαHRS	1:500	Endosomal Protein Involved in Sorting to Lysosome (Late Endosome)
Rat Anti-Bip	RaαBip	1:20	Endoplasmic Reticulum
Mouse Anti-Achaete	MαAc	1:4	Downstream Target of Wingless
Mouse Anti-Distalless	MαDll	1:500	Long Range Target of Wingless
Rat Anti-Cubitus Interruptus	RaαCi	1:20	Anterior Compartment (Segment Polarity Gene)
Guinea Pig Anti-Senseless	GpαSens	1:1000	Proneural Protein

Rat Anti-ELAV	RaαELAV	1:10	Pan-Neuronal Cell Body
Mouse Anti-Cut	MαCut	1:10	Cell Fate Regulator
Mouse Anti-Engrailed	MαEn	1:4	Posterior Compartment
Mouse Anti-BP102	MαBP102	1:10	CNS Axons
Chicken Anti-β-Galactosidase	ChαBGal	1:100	Hydrolase Enzyme

Secondary Antibody	**Abbreviation**	**Dilution**	**Fluorescence**
Anti-Green Fluorescent Protein A^{488}	αGFP A^{488}	1:1000	Green
Anti-Mouse A^{488}	αM A^{488}	1:500	Green
Anti-Mouse A^{568}	αM A^{568}	1:500	Red
Anti-Mouse A^{647}	αM A^{647}	1:500	Blue
Anti-Rabbit A^{488}	αRb A^{488}	1:500	Green
Anti-Rabbit A^{568}	αRb A^{568}	1:500	Red
Anti-Guinea Pig A^{549}	αGp A^{549}	1:500	Green
Anti-Guinea Pig A^{647}	αGp A^{647}	1:500	Blue
Anti-Rat A^{647}	αRa A^{647}	1:500	Blue
Anti-Phalloidin A^{647}	αPhalloidin A^{647}	1:100	Blue (Actin Cytoskeleton)
Anti-Chicken A^{488}	αCh A^{488}	1:500	Green

Appendix B

PRIMERS

Several experiments utilized primers designed to cover the *atg18* gene region and additional actin control primers. This image is to serve as a visual reference for expected results of these experiments. The chart following this figure lists product sizes in number of base pairs expected for each set of primer pairs.

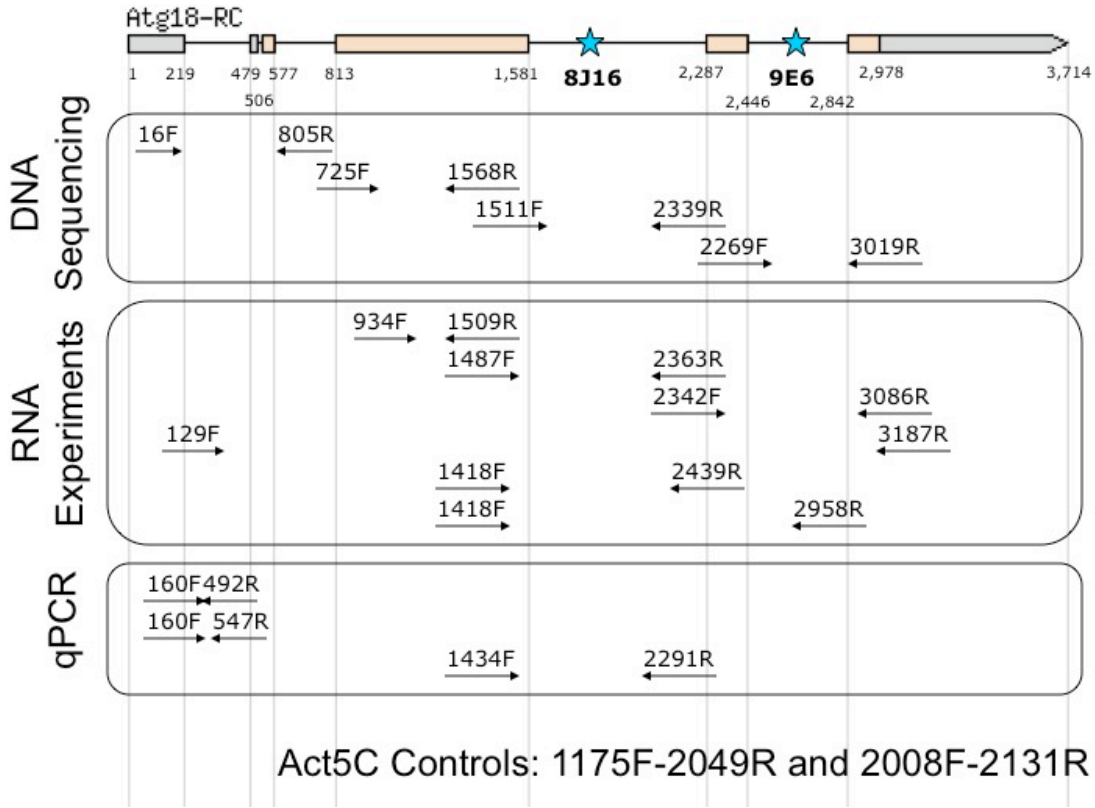

Primer Pairs	Expected Product
16F-805R	790
725F-1568R	844
1511F-2339R	829
2269F-3019R	751
934F-1509R	576
1487F-2363R	171
2342F-3086R	349
129F-3187R	1461
1418F-2439R	316
1418F-2958R	438
160F-492R	73
160F-547R	128
1434F-2291R	152
1175F-2049R (Act5C)	282
2008F-2131R (Act5C)	124

The following table includes sequences of the primers used to perform the initial sequencing of the *atg18* gene region.

Primer	**Sequence**
16F	TGTGGGTGCTGGTGTGTGTGC
805R	GGTGGAAAGTGTGAGTGGGTTGGC
725F	TGTATGAGTCATTGTTTCTGCAAAGCG
1568R	TCGCTCGACTGCTTGCTGCC
1511F	GGCTGGATCGCAGTGCCACG
2339R	GCGTGGGCAGGTAGCTGGTG
2269F	TCTACTCTCTCATGCAAGTTACTCGTTT
3019R	TGGGATGTGTGTAAGTGTGAAGTGTGT

Appendix C

SOLUTIONS

- **5X PEM**: 0.1 M pipes, 2 mM EGTA, 1mM $MgSO_4$ pH adjusted to 6.95 with concentrated HCl and stored at 4°C

- **PEM-FA**: 5X PEM (final 1X), 16% formaldehyde (4% final), distilled water

- **1X Phosphate Buffered Saline (PBS)**: 10 mM phosphate (pH 7.4), 183 mM NaCl, 27 mM KCl

- **1X Phosphate Buffered Saline (PBT)**: 10 mM phosphate (pH 7.4), 138 mM NaCl, 27 mM KCl, 0.1% Triton-X 100, 0.1% BSA

- **50X Tris, Acetic Acid, EDTA (TAE) Stock Solution:** 242 g Tris Base (MW=121.1)**,** 57.1 mL Glacial Acetic Acid**,** 100 mL 0.5 M EDTA **(**mix Tris with stir bar to dissolve in 600 mL of ddH2O, add EDTA and Acetic Acid, bring final volume to 1 L with ddH2O, and store at room temperature). Dilute to working concentration (1X) using diH_2O.

- **Hoyer's Mounting Media:** 30 g gum Arabic dissolved in 50 mL H_2O under a fume hood and heated to 60°C. 200 g chloral hydrate is slowly added and dissolved. 20 g glycerol is added, the mixture is centrifuged at 10,000xg, and the supernatant is filtered through glass wool (Selva & Stronach, 2007).

- **Fly Genomic DNA Solution A:** 0.1 M Tris-HCL, pH 9.0, 0.1 M EDTA, 1X SDS

- **Ethidium Bromide Solution:** 10 µl ethidium bromide (10 mg/ml) in 200 ml distilled water

Appendix D

DROSOPHILA CROSSES

Below is the series of crosses used to generate germline clone embryos used in the complementation analysis and staining experiments.

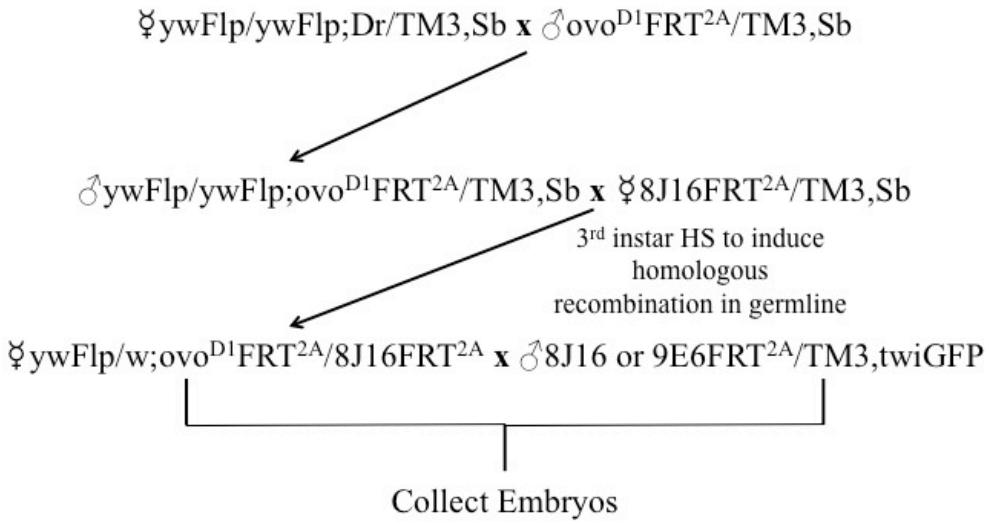

The figure below shows crosses designed to induce homologous recombination and create mitotic clones in the wing disc under the control of Gal4, a non-heat shock promoter.